Glycobiology vol. 17 no. 6 pp. 600–619, 2007
doi:10.1093/glycob/cwm015
Advance Access publication on February 9, 2007

N-glycans of recombinant human acid α-glucosidase expressed in the milk of transgenic rabbits

Susanne P Jongen[4], Gerrit J Gerwig[4], Bas R Leeflang[4], Kate Koles[2,4], Maurice LM Mannesse[5], Patrick HC van Berkel[3,5], Frank R Pieper[5], Marian A Kroos[6], Arnold JJ Reuser[6], Qun Zhou[7], Xiaoying Jin[7], Kate Zhang[7], Tim Edmunds[7], and Johannis P Kamerling[1,4]

[4]Bijvoet Center for Biomolecular Research, Department of Bio-Organic Chemistry, Utrecht University, Padualaan 8, NL-3584 CH Utrecht, The Netherlands; [5]Pharming Technologies BV, P.O. Box 451, NL-2300 AL Leiden, The Netherlands; [6]Department of Clinical Genetics, Erasmus MC, P.O. Box 1738, NL-3000 DR Rotterdam, The Netherlands; and [7]Genzyme Corporation, Framingham, MA 01701

Received on October 19, 2006; revised on February 2, 2007; accepted on February 3, 2007

Pompe disease is a lysosomal glycogen storage disorder characterized by acid α-glucosidase (GAA) deficiency. More than 110 different pathogenic mutations in the gene encoding GAA have been observed. Patients with this disease are being treated by intravenous injection of recombinant forms of the enzyme. Focusing on recombinant approaches to produce the enzyme means that specific attention has to be paid to the generated glycosylation patterns. Here, human GAA was expressed in the mammary gland of transgenic rabbits. The N-linked glycans of recombinant human GAA (rhAGLU), isolated from the rabbit milk, were released by peptide-N^4-(*N*-acetyl-β-glucosaminyl)asparagine amidase F. The N-glycan pool was fractionated and purified into individual components by a combination of anion-exchange, normal-phase, and *Sambucus nigra* agglutinin-affinity chromatography. The structures of the components were analyzed by 500 MHz one-dimensional and 600 MHz cryo two-dimensional (total correlation spectroscopy [TOCSY] nuclear Overhauser enhancement spectroscopy) ^{1}H nuclear magnetic resonance spectroscopy, combined with two-dimensional ^{31}P-filtered ^{1}H-^{1}H TOCSY spectroscopy, matrix-assisted laser desorption ionization time-of-flight mass spectrometry, and high-performance liquid chromatography (HPLC)-profiling of 2-aminobenzamide-labeled glycans combined with exoglycosidase digestions. The recombinant rabbit glycoprotein contained a broad array of different N-glycans, comprising oligomannose-, hybrid-, and complex-type structures. Part of the oligomannose-type glycans showed the presence of phospho-diester-bridged *N*-acetylglucosamine. For the complex-type glycans (partially) (α2-6)-sialylated (nearly only *N*-acetylneuraminic acid) diantennary structures were found; part of the structures were (α1-6)-core-fucosylated or (α1-3)-fucosylated in the upper antenna (Lewis x). Using HPLC-mass spectrometry of glycopeptides, information was generated with respect to the site-specific location of the various glycans.

Key words: N-glycosylation/recombinant human acid α-glucosidase/transgenic rabbit milk

Introduction

Pompe disease, also known as acid maltase deficiency, is a glycogen storage disease, GSD type II, and belongs to the family of inherited lysosomal storage disorders (Hirschhorn 2001). The disease is characterized by a major deficiency of acid α-glucosidase (1,4-α-D-glucan glucohydrolase; GAA; EC 3.2.1.3/20) and is caused by mutations in the GAA gene. Glycogen accumulates predominantly in heart, skeletal, and smooth muscle where it causes cellular damage. Loss of mobility and weakening of the respiratory function are the main clinical findings. Cardiac failure occurs in the most severe cases. Disease severity is related to the amount of residual GAA activity (Reuser et al. 1995). Infants born with a complete lack of enzyme activity have a maximum lifespan of 2 years (Van den Hout et al. 2003). The onset of symptoms in adults can be delayed till the sixth decade of life with only 5–25% of GAA activity.

Human GAA is synthesized as a 110-kDa single-chain precursor protein containing seven N-glycosylation sites (Asn-140, -233, -390, -470, -652, -882, and -925) (Hermans et al. 1993). Its transport from the endoplasmic reticulum via the Golgi network to the lysosomes is mediated by the mannose 6-phosphate receptor (MPR) (Hasilik and Neufeld 1980). In this process the lysosomal enzyme oligomannose-type N-glycans with mannose 6-phosphate groups are essential (Kaplan et al. 1977; Kornfeld 1986). In the late-endosomal/lysosomal compartments the precursor is proteolytically converted into a multipeptide complex (Moreland et al. 2005). A small amount of the precursor is transported to the plasma membrane, and secreted (Wisselaar et al. 1993).

Recently, enzyme replacement therapy by intravenous injection of GAA has demonstrated promising results in the treatment of Pompe disease (van den Hout et al. 2000; Winkel et al. 2004; Kishnani et al. 2006). As one of the possibilities for large-scale production of therapeutic enzyme, recombinant human acid α-glucosidase (rhAGLU) has been produced in the milk of transgenic rabbits (up to 8 mg/ml) (Bijvoet et al. 1999). The transgene construct consisted of the human GAA

[1]To whom correspondence should be addressed; e-mail: j.p.kamerling@chem.uu.nl
[2]Present address: Department of Biochemistry and Biophysics, Texas A&M University, 2128 TAMU, College Station, TX 77843-2128
[3]Present address: GenMab BV, Jenalaan 18d, NL-3584 CK Utrecht, The Netherlands

gene cloned behind the bovine αS1-casein gene promoter (Bijvoet et al. 1998). The purified rhAGLU has an apparent molecular mass of 110 kDa, comparable to the natural GAA precursor secreted in human urine (Oude Elferink et al. 1984). It has been tested in phase I and II trials in babies and older patients with positive results (van den Hout et al. 2000; van den Hout et al. 2001; Winkel et al. 2004).

At present the glycosylation machinery of the rabbit mammary gland is rather unexplored. Recent data have become available from detailed studies on human C1 inhibitor (Koles, van Berkel, Pieper, et al. 2004; Koles, van Berkel, Mannesse, et al. 2004) but, so far, glycosylation patterns of lysosomal enzymes have not been reported. In this study, a detailed analysis of the N-glycans of rhAGLU expressed in the milk of transgenic rabbits is presented, and the glycosylation pathway is discussed.

Results

General

Monosaccharide analysis (Kamerling and Vliegenthart 1989) of rhAGLU revealed the presence of Fuc, Man, Gal, GlcNAc, and sialic acid (Table I), and a carbohydrate content of 12% (by mass). GalNAc was not detected, indicating the absence of GalNAc(β1-4)GlcNAc-containing complex-/hybrid-type N-glycans, as well as the absence of conventional (mucin-type) O-glycans.

Release and fractionation of N-glycans of rhAGLU

The N-glycans of rhAGLU were completely released by peptide-N^4-(*N*-acetyl-β-glucosaminyl)asparagine amidase F (PNGase F) digestion, as determined by SDS-PAGE, and by monosaccharide analysis. On sodium dodecyl sulfate–polyacrylamide gel electrophoresis (SDS-PAGE), the native 110-kDa rhAGLU band migrated to a sharp 97-kDa band, after de-N-glycosylation (data not shown), in agreement with the de-N-glycosylation of seven Asn-sites. Monosaccharide analysis of the isolated N-glycan pool revealed a carbohydrate composition similar to that of the native glycoprotein (Table I). Sialic acid analysis of the glycan pool (and the native glycoprotein) showed, apart from Neu5Ac (97.9%), only trace amounts of Neu5Gc (0.2%) and Neu5,9Ac_2 (1.3%) (Figure 1).

Table I. Monosaccharide composition analysis of rhAGLU and derived N-glycan fractions

Monosaccharide	Molar ratio (Man taken as 3.0)				
	rhAGLU	N-glycan pool	**N0**	**N1**	**N2**
Fuc	0.3	0.4	–	0.4	0.4
Man	3.0	3.0	3.0	3.0	3.0
Gal	0.6	0.6	–	0.8	1.0
GlcNAc	2.7[a]	2.6	1.1	2.4	3.1
Sialic Acid (as Neu5Ac)	0.6	0.7	–	0.5	1.1

[a]Corrected for the stability of the GlcNAc-Asn linkage under the applied conditions.

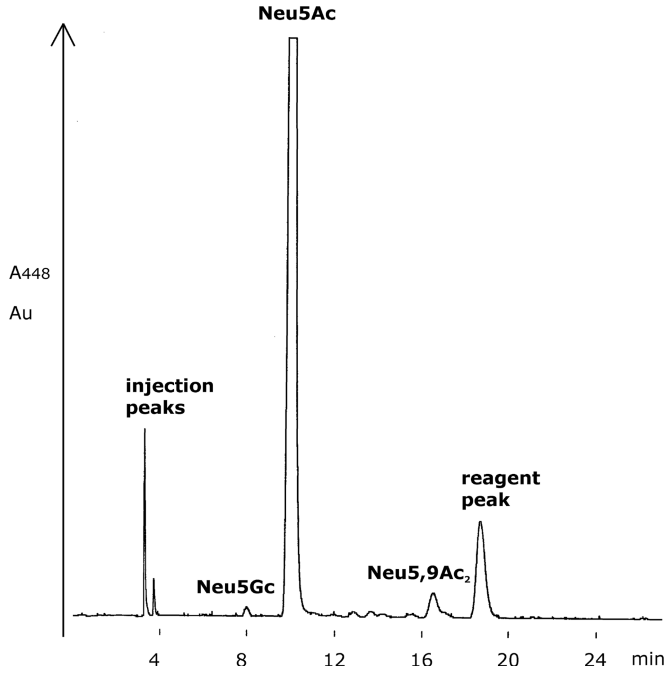

Fig. 1. Sialic acid analysis using DMB derivatives of the rhAGLU N-glycan pool after enzymatic release with PNGase F.

1D ^{1}H Nuclear magnetic resonance (NMR) analysis of the glycan pool, i.e, inspection of the structural-reporter-group regions (Vliegenthart et al. 1983; Koles, van Berkel, Pieper, et al. 2004), demonstrated the presence of a mixture of oligomannose- and complex-type N-glycan structures (Figure 2A), as well as the occurrence of GlcNAc in a GlcNAc(α1-*P*)Man unit (GlcNAc H-1, δ 5.481, $J_{1,2} = 3.5$ Hz, $J_{1,P} = 7.1$ Hz) (Nimtz et al. 1995). Neu5Ac residues were exclusively (α2-6)-linked (Neu5Ac H-3e, δ 2.668; Neu5Ac H-3a, δ 1.718), whereas Fuc residues occurred in (α1-6) linkage to the Asn-bound GlcNAc residue [Fuc CH_3, δ 1.209 (αGlcNAc-**1**) and 1.221 (βGlcNAc-**1**)], and in (α1-3) linkage as part of an antennary Lewis x element (Fuc CH_3, δ 1.178).

Fractionation of the N-glycan pool (80%) on Resource Q fast protein liquid chromatography (FPLC anion-exchange chromatography) yielded three carbohydrate-positive fractions, having elution positions corresponding to neutral (17%), mono-charged (43%), and di-charged (40%) N-glycans, denoted **N0**, **N1,** and **N2**, respectively (Figure 3).

*Structural analysis of neutral N-glycans of **N0***

Monosaccharide analysis of neutral FPLC fraction **N0** showed the presence of Man and GlcNAc only (Table I), supporting the presence of neutral oligomannose-type N-glycans, thereby eliminating the presence of neutral hybrid- and/or complex-type N-glycans. Its ^{1}H NMR spectrum revealed only structural reporters typical of oligomannose-type structures ranging from $Man_5GlcNAc_2$ to $Man_8GlcNAc_2$ (data not shown). Matrix-assisted laser desorption ionization time-of-flight mass spectrometry (MALDI-TOF MS) analysis showed the presence of $Man_5GlcNAc_2$ to $Man_9GlcNAc_2$ ($[M + Na]^+$, m/z 1257 /major peak, 1419, 1581, 1743, and 1906 / very minor peak) (data not shown). High-performance liquid

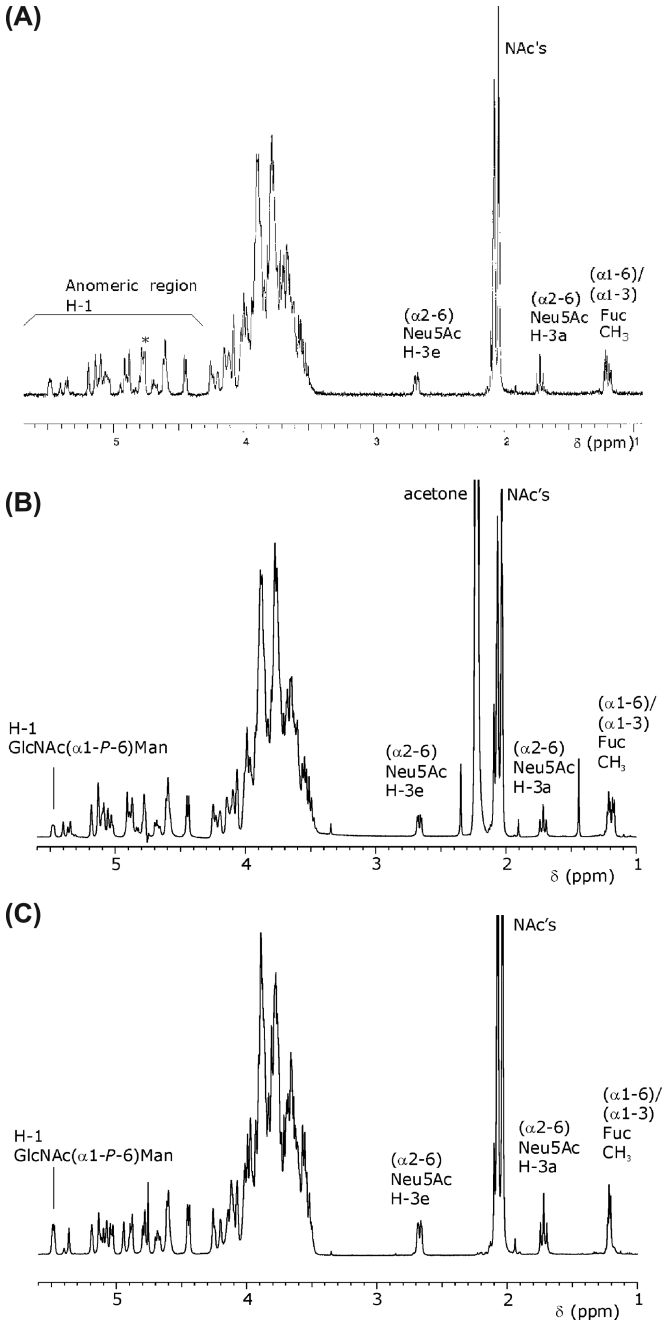

Fig. 2. One-dimensional 500 MHz ^{1}H NMR spectra of (**A**) the enzymatically released N-glycan pool of rhAGLU; (**B**) the mono-charged Resource Q fraction **N1**; (**C**) the di-charged Resource Q fraction **N2**. The peak marked by an asterisk is stemming from the ^{2}HO^{1}H signal.

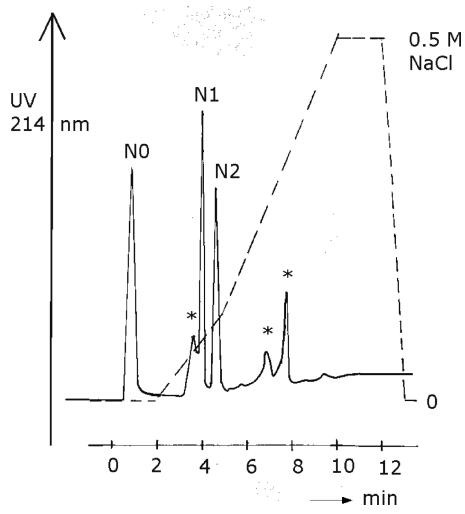

Fig. 3. Elution profile at 214 nm of the enzymatically-released N-glycan pool of rhAGLU on a Resource Q column. The column was first eluted with 8 ml water, followed by a linear concentration gradient of 0–25% (v/v) 0.5 M NaCl over 3 min, and by a steeper linear concentration gradient of 25–100% (v/v) 0.5 M NaCl over 5 min, at a flow rate of 4 ml/min. The fractions marked by an asterisk did not contain carbohydrate.

chromatography (HPLC) profiling of 2-aminobenzamide (2-AB) labeled fraction **N0** gave rise to five peaks, belonging to $Man_5GlcNAc_2$ (47%), $Man_6GlcNAc_2$ (27%), $Man_7GlcNAc_2$ (16%), $Man_8GlcNAc_2$ (8%), and $Man_9GlcNAc_2$ (2%) (data not shown).

Neutral FPLC fraction **N0** was further preparatively separated by HPLC on LiChrosorb-NH_2, yielding five peaks, denoted **N0.5**–**N0.9** (Figure 4A), belonging to $Man_5GlcNAc_2$ (44%), $Man_6GlcNAc_2$ (25%), $Man_7GlcNAc_2$ (18%), $Man_8GlcNAc_2$ (11%), and $Man_9GlcNAc_2$ (2%), respectively, as verified by MALDI-TOF MS.

HPLC subfractions **N0.5**–**N0.9** were further investigated by 1D ^{1}H NMR spectroscopy, and the structural-reporter-group data, typical for a series of oligomannose-type structures (Michalski et al. 1990; Stroop et al. 2000; Gutiérrez Gallego et al. 2004; Koles, van Berkel, Pieper, et al. 2004), are listed in Table II. Full structures, including the numbering of the Man and GlcNAc residues, are presented in Table III. Note that in case of oligomannose-type (and hybrid-type) N-glycans, the *N*-acetyl methyl signals of GlcNAc-**2** are generally observed at approximately δ 2.064. The ^{1}H NMR data of fraction **N0.5** correspond with a conventional $Man_5GlcNAc_2$ structure (cf. compounds QN2.1 in Stroop et al. 2000, and N0.2 in Koles, van Berkel, Pieper, et al. 2004). According to the ^{1}H NMR data of fraction **N0.6,** two isomers of $Man_6GlcNAc_2$, in a ratio of 21:4, occur. The major isomer **N0.6.1** is an extension of **N0.5** with Man-**C**, (α1-2)-linked to Man-**4** (Man6) (cf. compound QN2.2 in Stroop et al. 2000). The minor isomer **N0.6.2** is an extension of **N0.5** with Man-**D2**, (α1-2)-linked to Man-**A** (Man6′) (cf. compounds $N0.3.3_{2AB}$ in Koles, van Berkel, Pieper, et al. 2004, and $Man_6GlcNAc$ II in Michalski et al. 1990). For fraction **N0.7**, all three isomers of $Man_7GlcNAc_2$ as extensions of **N0.6.1** (Man6) were indicated to be present: **N0.7.1**, with Man-**D3** (α1-2)-linked to Man-**B** (Man7); **N0.7.2**, with Man-**D2** (α1-2)-linked to Man-**A** (Man7′); and **N0.7.3**, with Man-**D1** (α1-2)-linked to Man-**C** (Man7″) (cf. compounds QN2.3A and QN2.3B in Stroop et al. 2000, and Man7, Man7′, Man7″ in Gutiérrez Gallego et al. 2004); ratio 11:5:2. Similarly, for fraction **N0.8** all three conventional isomers of $Man_8GlcNAc_2$ are present: **N0.8.1**, with both Man-**D1** and Man-**D3** (Man8); **N0.8.2**, with both Man-**D2** and Man-**D3** (Man8′); and **N0.8.3**, with both Man-**D1** and Man-**D2** (Man8″) (cf. compounds $N0.4.5_{2AB}$ in Koles, van Berkel, Pieper, et al. 2004, QN2.4 in Stroop et al. 2000, and

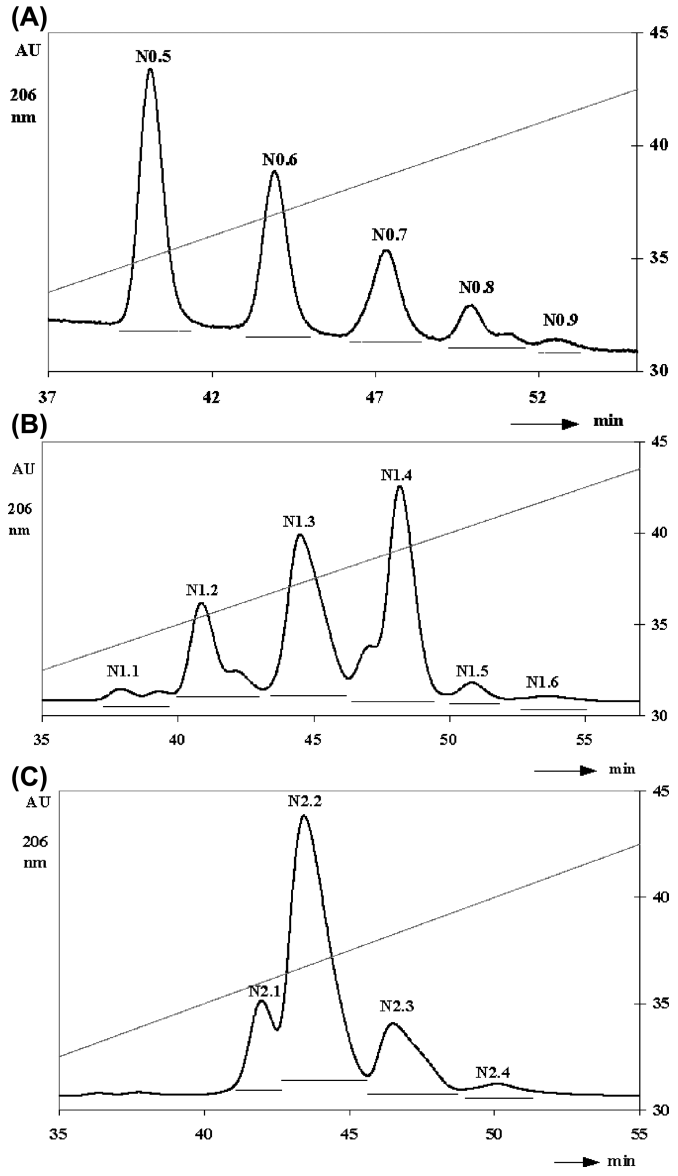

Fig. 4. Elution profile at 206 nm of (**A**) the neutral Resource Q fraction **N0** on a LiChrosorb-NH_2 column. The column was eluted with a linear gradient of 20–45% (v/v) water in acetonitrile for 50 min at a flow rate of 2 ml/min; (**B**) the mono-charged Resource Q fraction **N1** on a LiChrosorb-NH_2 column. A 50-min gradient of 10 mM potassium phosphate buffer, pH 6.5, in acetonitrile (20–45%, v/v) was used at a flow rate of 2 ml/min; (**C**) the di-charged Resource Q fraction **N2** on a LiChrosorb-NH_2 column. A 50-min gradient of 10 mM potassium phosphate buffer, pH 6.5, in acetonitrile (20–45%, v/v) was used at a flow rate of 2 ml/min.

$Man_8GlcNAc$ in Michalski et al. 1990); ratio 1:10:1. The amount of fraction **N0.9** was too low for NMR analysis. HPLC profiling studies on the 2-AB labeled fractions **N0.5**–**N0.9** confirmed the oligomannose-type structures $Man_5GlcNAc_2$-$Man_9GlcNAc_2$, as found in the NMR and MALDI-TOF MS analyses (Guile et al. 1996; Rudd and Dwek 1997).

*Structural analysis of mono-charged N-glycans of **N1***

Monosaccharide analysis of mono-charged FPLC fraction **N1** showed comparable data with those obtained for the N-glycan pool (Table I). Its ^{1}H NMR spectrum (Figure 2B) is similar to that of the N-glycan pool (Figure 2A), including the Neu5Ac(α2-6), Fuc(α1-6), Fuc(α1-3), and GlcNAc (α1-*P*)Man structural-reporter groups. It should be noted that in complex-type N-glycans an (α1-6)-fucosylated *N*,*N*′-diacetylchitobiose core element is recognized from the GlcNAc-**2** H-1 and NAc signals at δ 4.66–4.67 and 2.09–2.10, respectively, together with the set of Fuc H-1, CH_3, and H-5 signals at δ 4.89–4.91, 1.21–1.22, and 4.08–4.13, respectively. The nonfucosylated *N*,*N*′-diacetylchitobiose unit is recognized from the GlcNAc-**2** H-1 and NAc signals at δ 4.60–4.61 and approximately 2.081, respectively (Hård et al. 1992). Additionally, the presence of (α2-6)-linked Neu5Ac is reflected by methylene signals at δ 2.67 (H-3e) and 1.70–1.72 (H-3a), and the presence of a Lewis x determinant by the set of Fuc H-1, CH_3, and H-5 signals at δ 5.11–5.13, 1.17–1.18, and 4.83–4.84, respectively (Kamerling and Vliegenthart 1992).

Mono-charged FPLC fraction **N1** was further preparatively separated by HPLC on LiChrosorb-NH_2, yielding six fractions denoted **N1.1**–**N1.6** (Figure 4B). Screening of the various fractions by ^{1}H NMR spectroscopy showed for **N1.2**, **N1.3**, and **N1.4** complex mixtures, partially due to the presence of both Neu5Ac and phosphate residues. In order to separate (α2-6)-sialylated glycans from nonsialylated glycans, these HPLC fractions were subfractionated by lectin affinity chromatography on agarose-bound elderberry bark lectin (*Sambucus nigra* agglutinin, SNA). After loading, nonsialylated glycans were eluted with phosphate buffered saline (PBS) buffer as unbound (flow-through) fractions, coded **U**. Then, (α2-6)-sialylated glycans (bound fractions), coded **B**, were eluted with ethylenediamine (EDA). Subsequent elution with 50 mM lactose did not yield additional glycan material. The various **U** and **B** fractions were investigated by ^{1}H NMR spectroscopy, and the structural-reporter-group data are listed in Tables IV and V, respectively. Fractions **N1.1** (Table V) and **N1.6** contained no structural-reporter groups indicative for phosphorylation, so no further subfractionations were applied. Fraction **N1.5** did not contain enough material for further analysis. Full structures, including the numbering of the various residues, are depicted in Table VI.

MALDI-TOF MS analysis of **N1.1** revealed pseudomolecular ions at m/z 1789.94 and 1643.85, correlating with the $[M\text{-}H + 2K]^+$ adducts of $Neu5Ac_1Hex_4Fuc_1GlcNAc_3$ (M = 1789.55) and $Neu5Ac_1Hex_4GlcNAc_3$ (M = 1643.48), respectively. ^{1}H NMR analysis indicated the presence of an (α1-3) mono-antennary, mono-(α2-6)-sialylated complex-type N-glycan (Tables V and VI). The core GlcNAc-**1** residue is only partially (α1-6)-fucosylated (cf. structure N1.4 in Koles, van Berkel, Pieper, et al. 2004). HPLC profiling and exoglycosidase studies on the 2-AB labeled material confirmed the occurrence of both structures (data not shown).

MALDI-TOF MS analysis of **N1.2U**, **N1.3U**, and **N1.4U** revealed pseudomolecular ions at m/z 1724.65, 1886.92, and 2049.17, respectively, correlating with the $[M\text{-}H + 2Na]^+$ adducts of $Hex_6PGlcNAc_3$ (M = 1724.50), $Hex_7PGlcNAc_3$ (M = 1886.56), and $Hex_8PGlcNAc_3$ (M = 2048.61), respectively.

^{1}H NMR analysis of fraction **N1.2U** indicated the presence of $Man_6GlcNAc_2$ structure **N0.6.1** (Man6), extended with a GlcNAc(α1-*P*) element. The presence of the GlcNAc(α1-*P*) element is reflected by the occurrence of the GlcNAc H-1

Table II. ^{1}H Chemical shifts of the structural-reporter-group protons of the constituent monosaccharides of neutral oligomannose-type N-glycans, liberated from rhAGLU

Reporter group	Residue	Chemical shifts in ppm								
		 **N0.5**	 **N0.6.1**	 **N0.6.2**	 **N0.7.1**	 **N0.7.2**	 **N0.7.3**	 **N0.8.1**	 **N0.8.2**	 **N0.8.3**
H-1	GlcNAc-**1**α	5.188	5.187	5.187	5.187	5.187	5.187	5.187	5.187	5.187
	GlcNAc-**2**	4.60	4.60	4.60	4.60	4.60	4.60	4.60	4.60	4.60
	Man-**4**	5.094	5.347	5.093	5.345	5.345	5.345	5.345	5.345	5.345
	Man-**4′**	4.871	4.872	4.872	4.869	4.869	4.869	4.869	4.869	4.869
	Man-**A**	5.094	5.093	5.404	5.090	5.404	5.090	5.091	5.404	5.412
	Man-**B**	4.907	4.908	4.908	5.146	4.907	4.907	5.143	5.143	4.91
	Man-**C**		5.052		5.054	5.054	5.305	5.31	5.059	5.31
	Man-**D1**						5.042	5.040		5.040
	Man-**D2**			5.052		5.054			5.059	5.059
	Man-**D3**				5.042			5.040	5.040	
H-2	Man-**3**	4.253	4.232	4.252	4.232	4.232	4.232	4.231	4.231	4.231
	Man-**4**	4.076	4.115	4.067	4.11	4.11	4.11	4.11	4.123	4.11
	Man-**4′**	4.147	4.146	4.146	4.148	4.148	4.148	4.156	4.156	4.156
	Man-**A**	4.067	4.067	4.093	4.068	4.093	4.068	4.07	4.09	4.09
	Man-**B**	3.982	3.983	3.983	4.017	3.993	3.993	4.02	4.02	3.99
	Man-**C**		4.067		4.068	4.068	4.11	4.11	4.07	4.11
	Man-**D1**						4.068	4.07		4.07
	Man-**D2**			4.067		4.068			4.07	4.07
	Man-**D3**				4.068			4.07	4.07	
NAc	GlcNAc-**1**	2.037	2.037	2.037	2.037	2.037	2.037	2.037	2.037	2.037
	GlcNAc-**2**	2.064	2.064	2.064	2.064	2.064	2.064	2.068	2.068	2.068

Chemical shifts are given relative to internal acetone (δ 2.225) in $^{2}H_2O$ at p^{2}H 7 and 300 K. Compounds are represented by short-hand symbolic notation: ◆, Man; ●, GlcNAc; α stands for the anomeric configuration of GlcNAc-**1**. For numbering of the oligosaccharide residues, see Table III, **N0.9.**

Table III. Relative amounts and structures of the identified neutral oligomannose-type N-glycans of rhAGLU

Code	Glycan structure		% of glycan pool	% per charge state
N0.5	Man5	Man(α1-6) \ Man(α1-6) / \ Man(α1-3) Man(β1-4)GlcNAc(β1-4)GlcNAc / Man(α1-3)	7	44
N0.6.1	Man6	Man(α1-6) \ Man(α1-6) / \ Man(α1-3) Man(β1-4)GlcNAc(β1-4)GlcNAc / Man(α1-2)Man(α1-3)	3	21
N0.6.2	Man6′	Man(α1-6) \ Man(α1-6) / \ Man(α1-2)Man(α1-3) Man(β1-4)GlcNAc(β1-4)GlcNAc / Man(α1-3)	1	4
N0.7.1	Man7	Man(α1-2)Man(α1-6) \ Man(α1-6) / \ Man(α1-3) Man(β1-4)GlcNAc(β1-4)GlcNAc / Man(α1-2)Man(α1-3)	2	11
N0.7.2	Man7′	Man(α1-6) \ Man(α1-6) / \ Man(α1-2)Man(α1-3) Man(β1-4)GlcNAc(β1-4)GlcNAc / Man(α1-2)Man(α1-3)	1	5
N0.7.3	Man7″	Man(α1-6) \ Man(α1-6) / \ Man(α1-3) Man(β1-4)GlcNAc(β1-4)GlcNAc / Man(α1-2)Man(α1-2)Man(α1-3)	<1	2
N0.8.1	Man8	Man(α1-2)Man(α1-6) \ Man(α1-6) / \ Man(α1-3) Man(β1-4)GlcNAc(β1-4)GlcNAc / Man(α1-2)Man(α1-2)Man(α1-3)	≪1	<1
N0.8.2	Man8′	Man(α1-2)Man(α1-6) \ Man(α1-6) / \ Man(α1-2)Man(α1-3) Man(β1-4)GlcNAc(β1-4)GlcNAc / Man(α1-2)Man(α1-3)	2	10
N0.8.3	Man8″	Man(α1-6) \ Man(α1-6) / \ Man(α1-2)Man(α1-3) Man(β1-4)GlcNAc(β1-4)GlcNAc / Man(α1-2)Man(α1-2)Man(α1-3)	≪ 1	<1

Continued

Table III. *Continued*

Code	Glycan structure	% of glycan pool	% per charge state
N0.9	Man9	<1	2

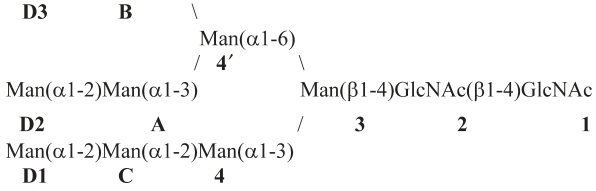

and NAc signals at δ 5.482 and 2.074, respectively (Figure 5A). Going from **N0.6.1** to **N1.2U**, an upfield shift is observed for Man-**C** H-1 (Δδ −0.030 ppm) (Figure 6), and a downfield shift for Man-**C** H-2 (Δδ +0.012 ppm). Furthermore, a downfield shift is observed for Man-**4** H-1 (Δδ +0.020 ppm), and an upfield shift for Man-**4** H-2 (Δδ −0.017 ppm). The structural-reporter-group data of **N1.2U** fit those of the earlier reported GlcNAc-*P*-$Man_6GlcNAc_2$ structure, having a GlcNAc(α1-*P*-6)Man-**C** element, derived from BHK-21-expressed EPO (Nimtz et al. 1995). Here, the H-6a/H-6b signals of the phosphorylated Man-**C** residue have shifted out of the bulk region into the Man H-2 region, thereby complicating the spectrum at δ 4.00–4.02 ppm. It should be noted that also Man-**B** H-2 is influenced by Δδ −0.017 ppm probably demonstrating, by comparing **N0.6.1** and **N1.2U**, the change in microenvironment. For a confirmation of the GlcNAc(α1-*P*-6)Man linkage using ^{31}P-filtered 2D ^{1}H-^{1}H total correlation spectroscopy (TOCSY), see the analysis of **N2.2U**, described in *Structural analysis of di-charged N-glycans of N2*. Previously, it has been shown that going from the trisaccharide Man-**D1**(α1-2)Man-**C**(α1-2)Man-**4** to the GlcNAc-phosphorylated trisaccharide Man-**D1**(α1-2)[GlcNAc(α1-*P*-6)]Man-**C**(α1-2)Man-**4**, Man-**C** shows an upfield shift for H-1 (Δδ −0.065 ppm) and a downfield shift for H-2 (Δδ +0.017 ppm) (de Waard et al. 1989).

^{1}H NMR analysis of fraction **N1.3U** revealed the occurrence of three GlcNAc-*P*-$Man_7GlcNAc_2$ structures derived from **N0.7.1** (Man7) and **N0.7.2** (Man7′), by extension with a GlcNAc(α1-*P*) element (GlcNAc H-1, δ 5.484; GlcNAc NAc, δ 2.076). Going from **N0.7.2** to **N1.3U.1**, an upfield shift is detected for Man-**C** H-1 (Δδ −0.032 ppm). The observed downfield shift for Man-**B** H-1 (Δδ +0.02 ppm) is not due to a GlcNAc-phosphorylation at Man-**B**, as substitution of this residue gives rise to upfield shifts (see e.g., **N1.3U.3**). **N1.3U.2** is an extension of **N0.7.1** with a GlcNAc(α1-*P*)Man-**C** unit, indicated by the upfield shift for Man-**C** H-1 (Δδ −0.032 ppm) (compare with **N1.2U**). Going from **N0.7.1** to **N1.3U.3**, an upfield shift is detected for Man-**B** H-1 (Δδ −0.037 ppm). Taking into account the NMR data for the GlcNAc(α1-*P*-6) element (Nimtz et al. 1995) as well as the Man-**B** H-1 upfield shift, a GlcNAc(α1-*P*-6)Man-**B** unit is suggested, yielding a Man-**D3**(α1-2)[GlcNAc(α1-*P*-6)]Man-**B**(α1-6)Man-**4**′ element in **N1.3U.3** (for further details about Man-**B** GlcNAc-phosphorylation, see **N2.2U**).

The ^{1}H NMR spectrum of **N1.4U** showed the presence of $Man_8GlcNAc_2$ structure **N0.8.2** (Man8′), extended with a GlcNAc(α1-*P*) element (GlcNAc H-1, δ 5.483; GlcNAc NAc, δ 2.075) (Figure 5B). Going from **N0.8.2** to **N1.4U**, upfield shifts are seen for Man-**B** H-1 (Δδ −0.044 ppm) and Man-**D3** H-1 (Δδ −0.006 ppm), in agreement with the presence of a GlcNAc(α1-*P*-6)Man-**B** unit (see **N1.3U.3** and **N2.2U**).

HPLC profiling studies of the 2-AB labeled fractions **N1.2U**, **N1.3U**, and **N1.4U** before and after treatment with mild acid (removal of GlcNAc)/alkaline phosphatase (removal of phosphate) confirmed the presence of GlcNAc-phosphorylated $Man_6GlcNAc_2$, $Man_7GlcNAc_2$ and $Man_8GlcNAc_2$ structures, respectively.

MALDI-TOF MS analysis of fraction **N1.2B** showed pseudomolecular ions at m/z 1773.46 and 1919.54, corresponding with the $[M\text{-}H + 2Na]^+$ adducts of $Neu5Ac_1Hex_5GlcNAc_3$ ($M = 1773.58$) and $Neu5Ac_1Hex_5Fuc_1GlcNAc_3$ ($M = 1919.64$), respectively. The ^{1}H NMR spectrum of **N1.2B** reflected an (α2-6)-sialylated hybrid-type N-glycan with a Man-**A**(α1-3)Man-**4**′(α1-6) unit (Man-**A** H-1, δ 5.106; Man-**4**′ H-1, δ 4.896; cf. N1.5B in Koles, van Berkel, Pieper, et al. 2004); the core GlcNAc-**1** residue is only (α1-6)-fucosylated for 60%. These results are in agreement with HPLC profiling/exo-glycosidase studies of the 2-AB labeled fraction **N1.2B**.

MALDI-TOF MS analysis of fraction **N1.3B** revealed pseudomolecular ions at m/z 2123.72 and 2437.83, corresponding with the $[M\text{-}H + 2Na]^+$ adduct of $Neu5Ac_1Hex_5Fuc_1GlcNAc_4$ ($M = 2122.72$) and the $[M\text{-}2H + 3Na]^+$ adduct of $Neu5Ac_2Hex_5Fuc_1GlcNAc_4$ ($M = 2435.80$), respectively. The ^{1}H NMR spectrum of **N1.3B** revealed the presence of a mixture of a monosialylated (<5%) and a disialylated (>95%) diantennary chain with core (α1-6)-fucosylation. For the monosialylated form, only the (α1-3) arm is sialylated (Man-**4** H-1, δ 5.133; cf. N1.3 in Koles, van Berkel, Pieper, et al. 2004; Q1.2 in van Rooijen et al. 1998). The disialylated form is identical to the compound in fraction **N2.2B**, indicating an incomplete subfractionation. Due to its low amount, the structural-reporter-group signals of the monosialylated compound are not included in Table V. The various results are in agreement with HPLC profiling/exo-glycosidase studies of the 2-AB labeled fraction **N1.3B**.

MALDI-TOF MS analysis of fraction **N1.4B** showed a major pseudomolecular ion at m/z 2270.09, corresponding with the $[M\text{-}H + 2Na]^+$ adduct of $Neu5Ac_1Hex_5Fuc_2GlcNAc_4$ ($M = 2268.78$). ^{1}H NMR analysis indicated the major presence (>90%) of an (α1-6)-fucosylated diantennary N-glycan, (α2-6)-sialylated in the (α1-3) arm and with a Lewis x determinant in the (α1-6) arm (Fuc H-1,

Table IV. ^{1}H Chemical shifts of the structural-reporter-group protons of the constituent monosaccharides of the phosphorylated oligomannose-type N-glycans, liberated from rhAGLU

Reporter group	Residue	Chemicals shifts in ppm							
						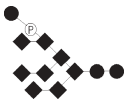	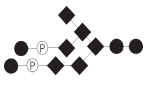	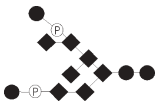	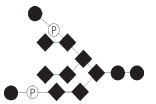
		N1.2U	**N1.3U.1**	**N1.3U.2**	**N1.3U.3**	**N1.4U**	**N2.1U**	**N2.2U**	**N2.3U**
H-1	GlcNAc-**1α**	5.190	5.189	5.189	5.189	5.188	5.191	5.194	5.195
	GlcNAc-**2**	4.594	4.594	4.594	4.594	4.597	4.59	4.620	4.60
	Man-**4**	5.367	5.367	5.367	5.349	5.346	5.362	5.362	5.365
	Man-**4′**	4.876	4.871	4.871	4.871	4.868	4.875	4.877	4.874
	Man-**A**	5.090	5.406	5.085	5.085	5.403	5.067	5.072	5.402
	Man-**B**	4.913	4.93	5.148	5.109	5.099	4.903	5.096	5.082
	Man-**C**	5.022	5.022	5.022	5.058	5.061	5.021	5.025	5.026
	Man-**D1**								
	Man-**D2**		5.058			5.061			5.068
	Man-**D3**			5.042	5.042	5.034		5.043	5.048
	GlcNAc-*P*	5.482	5.484	5.484	5.484	5.483	5.479	5.482	5.482
H-2	Man-**3**	4.234	4.234	4.234	4.234	4.231	4.238	4.239	4.242
	Man-**4**	4.098	nd	nd	nd	4.128	4.107	4.119	nd
	Man-**4′**	4.150	nd	nd	nd	4.149	4.137	4.144	4.154
	Man-**A**	4.068	nd	nd	nd	4.069	nd	4.069	nd
	Man-**B**	4.000	nd	nd	nd	4.018	nd	4.019	nd
	Man-**C**	4.079	nd	nd	nd	4.071	nd	4.071	nd
	Man-**D1**								
	Man-**D2**		nd			4.071			nd
	Man-**D3**			nd	nd	4.071		4.071	nd
NAc	GlcNAc-**1**	2.037	2.037	2.037	2.037	2.037	2.037	2.037	2.037
	GlcNAc-**2**	2.063	2.065	2.065	2.065	2.068	2.065	2.064	2.069
	GlcNAc-*P*	2.074	2.076	2.076	2.076	2.075	2.077	2.076	2.076

Chemical shifts are given relative to internal acetone (δ 2.225) in $^{2}H_2O$ at p^{2}H 7 and 300 K. Compounds are represented by short-hand symbolic notation: ◆, Man; ●, GlcNAc; Ⓟ, phosphate; nd, not determined; α stands for the anomeric configuration of GlcNAc-**1**. For numbering of the oligosaccharide residues, see Table III, **N0.9.**

Table V. ^{1}H Chemical shifts of structural-reporter-group protons of the constituent monosaccharides of the sialylated hybrid- and complex-type N-glycans, liberated from rhAGLU

Reporter group	Residue	Chemicals shifts in ppm					
							
		N1.1	**N1.2B**	**N1.4B**	**N2.1B**	**N2.2B**	**N2.3B**
H-1	GlcNAc-**1α**	5.191/5.181	5.187	5.182	5.190	5.182	5.189
	Man-**4**	5.137	5.137	5.137	5.134	5.134	5.123
	Man-**4′**	4.919	4.896	4.914	4.949	4.942	4.876
	GlcNAc-**5**	4.603	4.605	4.608	4.606	4.605	4.605
	GlcNAc-**5′**			4.589	4.606	4.605	
	Gal-**6**	4.445	4.445	4.448	4.446	4.446	4.443
	Gal-**6′**			4.448	4.446	4.446	
	Man-**A**		5.106				5.079
	Man-**B**						5.113
	Man-**D3**						5.037
	GlcNAc-*P*						5.484
	Fuc(α1-6)$^{\alpha}$	4.89	4.89	4.885		4.893	
	Fuc(α1-6)$^{\beta}$	4.89	4.89	4.893		4.893	
	Fuc(α1-3)			5.132			
H-2	Man-**3**	4.257	4.248	4.259	4.256	4.258	4.254
	Man-**4**	4.195	4.199	4.195	4.197	4.198	4.208
	Man-**4′**	nd	4.137	4.096	4.119	4.115	4.142
	Man-**A**		4.066				4.071
H-3a	Neu5Ac	1.718	1.717	1.719	1.719	1.719	1.720
H-3e	Neu5Ac	2.669	2.669	2.669	2.671	2.671	2.669
H-5	Fuc(α1-3)			4.835			
CH_3	Fuc(α1-6)$^{\alpha}$	1.208	1.207	1.210		1.209	
	Fuc(α1-6)$^{\beta}$	1.220	1.218	1.221		1.221	
	Fuc(α1-3)			1.178			
NAc	GlcNAc-**1**	2.037	2.037	2.038	2.038	2.038	2.037
	GlcNAc-**2**	2.077/2.092	2.066/2.094	2.09[a]	2.083	2.098	2.064
	GlcNAc-**5**	2.068	2.066	2.068	2.068	2.068	2.064
	GlcNAc-**5′**			2.042	2.068	2.068	
	GlcNAc-*P*						2.079
	Neu5Ac	2.029	2.029	2.030	2.030	2.030	2.030

Chemical shifts are given relative to internal acetone (δ 2.225) in $^{2}H_2O$ at p^{2}H 7 and 300 K. Compounds are represented by short-hand symbolic notation: ◆, Man; ●, GlcNAc; ■, Gal; □, Fuc; ○, Neu5Ac(α2-6); Ⓟ, phosphate; nd, not determined, α and β stand for the anomeric configuration of GlcNAc-**1**. For numbering of the oligosaccharide residues, see Table VI, **N2.1B**, and Table III, **N0.9**. [a]less accurate due to side band spinning overlap of acetone.

Table VI. Relative amounts and structures of the identified mono- and di-charged N-glycans of rhAGLU

Code	Glycan structure	% of glycan pool	% per charge state
N1.1	Man(α1-6) [Fuc(α1-6)] \ \ Man(β1-4)GlcNAc(β1-4)GlcNAc / Neu5Ac(α2-6)Gal(β1-4)GlcNAc(β1-2)Man(α1-3)	1	<3
N1.2U	Man(α1-6) \ Man(α1-6) / \ Man(α1-3) Man(β1-4)GlcNAc(β1-4)GlcNAc / GlcNAc(α1-*P*-6)Man(α1-2)Man(α1-3)	4	10
N1.2B	Man(α1-6) [Fuc(α1-6)] / \ \ Man(α1-3) Man(β1-4)GlcNAc(β1-4)GlcNAc / Neu5Ac(α2-6)Gal(β1-4)GlcNAc(β1-2)Man(α1-3)	2	5
N1.3U.1	Man(α1-6) \ Man(α1-6) / \ Man(α1-2)Man(α1-3) Man(β1-4)GlcNAc(β1-4)GlcNAc / GlcNAc(α1-*P*-6)Man(α1-2)Man(α1-3)		
N1.3U.2	Man(α1-2)Man(α1-6) \ Man(α1-6) / \ Man(α1-3) Man(β1-4)GlcNAc(β1-4)GlcNAc / GlcNAc(α1-*P*-6)Man(α1-2)Man(α1-3)	12	28
N1.3U.3	GlcNAc(α1-*P*-6) \ Man(α1-2)Man(α1-6) \ Man(α1-6) / \ Man(α1-3) Man(β1-4)GlcNAc(β1-4)GlcNAc / Man(α1-2)Man(α1-3)		
N1.3B	Gal(β1-4)GlcNAc(β1-2)Man(α1-6) Fuc(α1-6) \ \ Man(β1-4)GlcNAc(β1-4)GlcNAc / Neu5Ac(α2-6)Gal(β1-4)GlcNAc(β1-2)Man(α1-3)	7	15
N1.4U	GlcNAc(α1-*P*-6) \ Man(α1-2)Man(α1-6) \ Man(α1-6) / \ Man(α1-2)Man(α1-3) Man(β1-4)GlcNAc(β1-4)GlcNAc / Man(α1-2)Man(α1-3)	3	8
N1.4B	Fuc(α1-3) \ Gal(β1-4)GlcNAc(β1-2)Man(α1-6) Fuc(α1-6) \ \ Man(β1-4)GlcNAc(β1-4)GlcNAc / Neu5Ac(α2-6)Gal(β1-4)GlcNAc(β1-2)Man(α1-3)	13	29

Continued

Table VI. *Continued*

Code	Glycan structure	% of glycan pool	% per charge state
N1.5	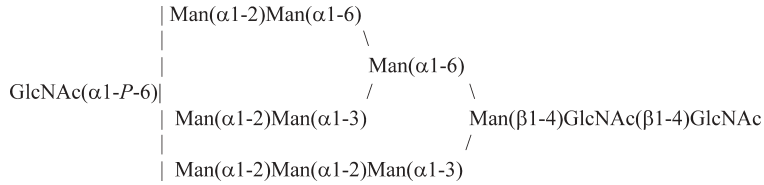	1	<2
N2.1U	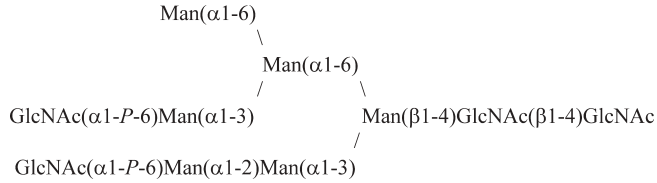	1	2
N2.1B	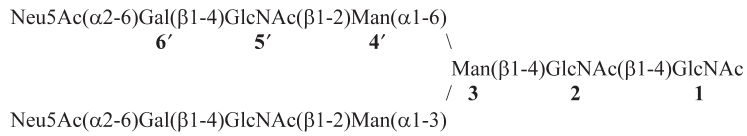	3	7
N2.2U	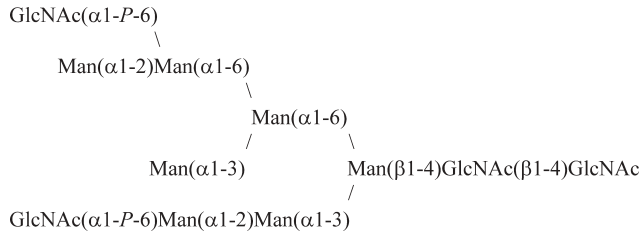	6	14
N2.2B	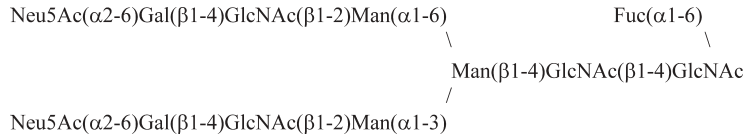	22	56
N2.3U	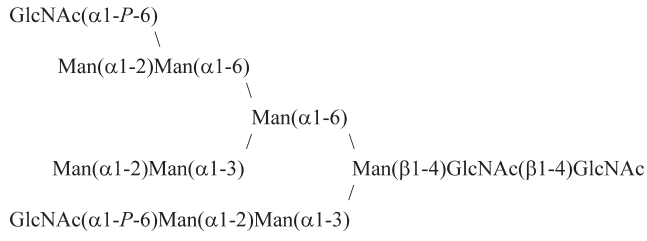	2	5
N2.3B	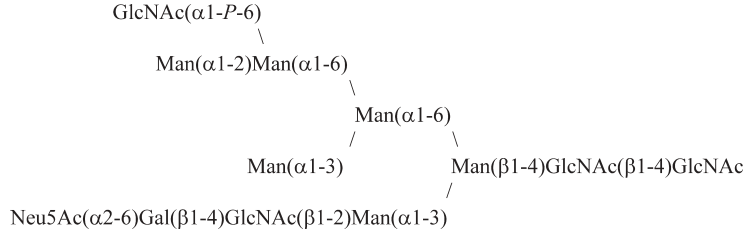	6	14
N2.4	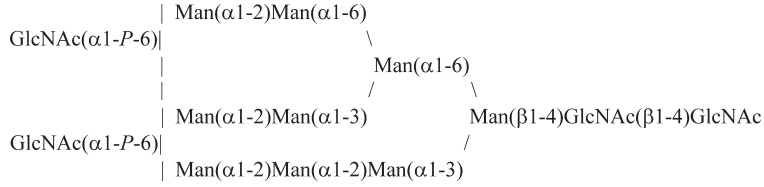	1	<2

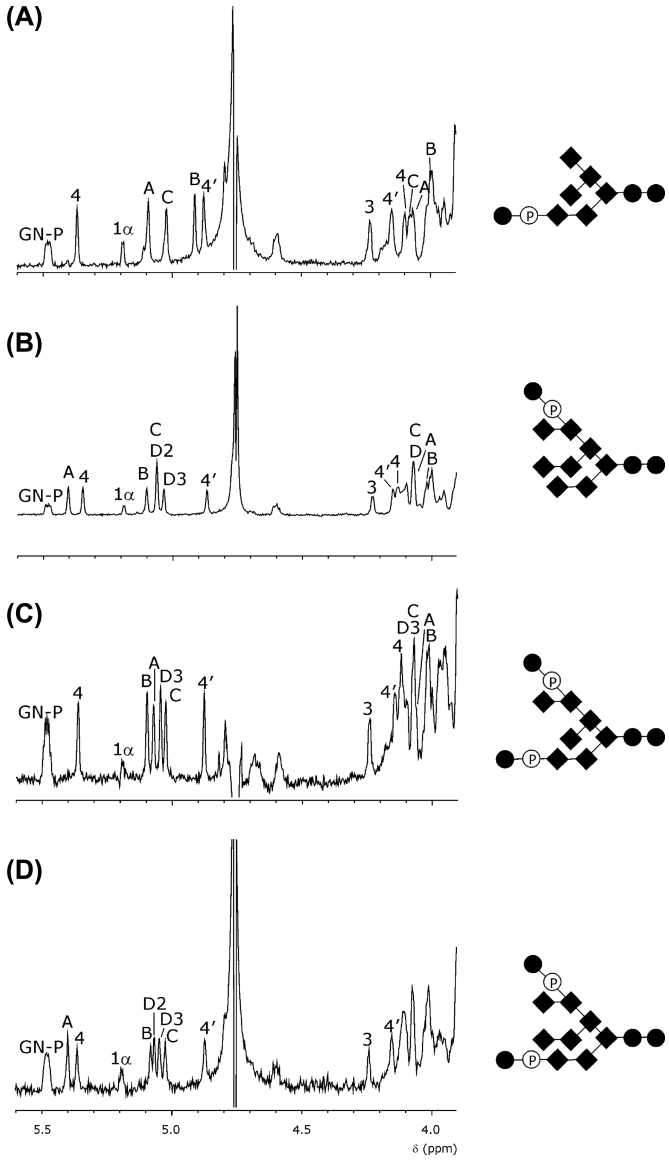

Fig. 5. Partial one-dimensional 500 MHz ^{1}H NMR spectra (H-1 region, δ 5.6-δ 4.4; H-2 region, δ 4.3-δ 3.9) of (**A**) fraction **N1.2U**; (**B**) fraction **N1.4U**; (**C**) fraction **N2.2U**; and (**D**) fraction **N2.3U**.

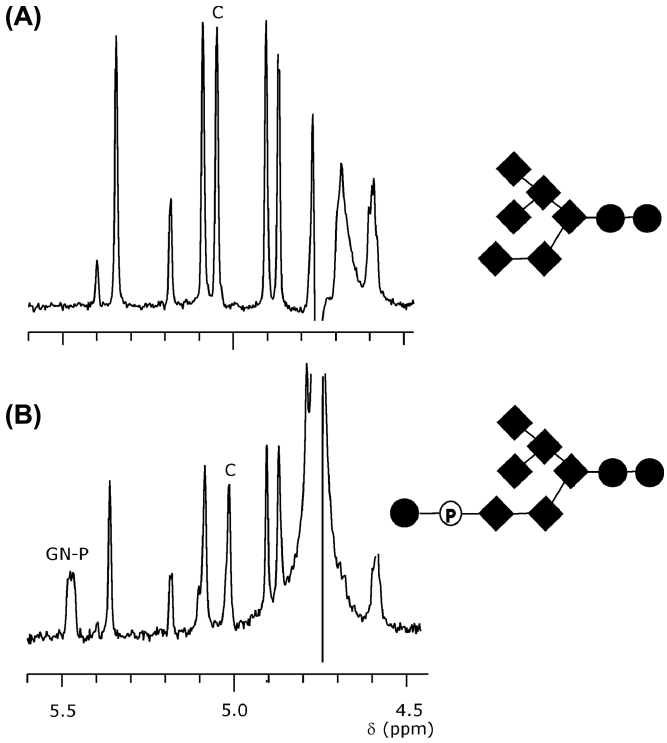

Fig. 6. Partial one-dimensional 500 MHz ^{1}H NMR spectra (H-1 region, δ 5.6-δ 4.4) of fractions **N0.6** [**N0.6.1** (major) and **N0.6.2** (minor)] (top) and **N1.2U** (bottom), indicating the shift at Man-**C** H-1 (**N0.6.1** → **N1.2U**) resulting from GlcNAc-phosphorylation, and the GlcNAc H-1 structural-reporter-group signal (GN-P).

δ 5.132; Fuc CH_3, δ 1.178; Man-4′ H-1, δ 4.914) (cf. structure N1.1 in Koles, van Berkel, Pieper, et al. 2004). HPLC profiling of the 2-AB labeled **N1.4B** on GlycoSep-N confirmed the presence of the difucosylated, monosialylated, diantennary N-glycan as the major structure.

MALDI-TOF MS analysis of **N1.5** revealed pseudomolecular ions at m/z 2302.28, 2464.38, and 2243.18, correlating with the $[M\text{-}H + 2K]^+$ adducts of $Neu5Ac_1Hex_5Fuc_2GlcNAc_4$ ($M = 2300.72$), $Neu5Ac_1Hex_6Fuc_2GlcNAc_4$ ($M = 2462.78$), and $Hex_9PGlcNAc_3$ ($M = 2242.61$), respectively. Taking into account the ^{1}H NMR data of fraction **N1.5**, it is proposed that $Neu5Ac_1Hex_5Fuc_2GlcNAc_4$ represents an (α1-6)-fucosylated, (α2-6)-monosialylated complex-type N-glycan with a Lewis x unit, $Neu5Ac_1Hex_6Fuc_2GlcNAc_4$ an (α1-6)-fucosylated, (α2-6)-monosialylated hybrid-type N-glycan with a Lewis x unit at the nonsialylated antenna, and $Hex_9PGlcNAc_3$ a GlcNAc-phosphorylated oligomannose-type N-glycan. The complex-type structure seems to stem from a chromatographic overlap with fraction **N1.4**.

MALDI-TOF MS analysis of **N1.6** revealed a pseudomolecular ion at m/z 2813.52, correlating with the $[M\text{-}H + 2K]^+$ adduct of $Neu5Ac_1Hex_6Fuc_3GlcNAc_5$ ($M = 2811.91$). Taking into account the ^{1}H NMR data, **N1.6** is suggested to be a triantennary (α1-6)-fucosylated, (α2-6)-monosialylated N-glycan with Lewis x epitopes at the nonsialylated antennae.

Structural analysis of di-charged N-glycans of N2

Monosaccharide analysis of di-charged FPLC fraction **N2** revealed only a gradual difference with that of fraction **N1** (Table I). Its ^{1}H NMR spectrum (Figure 2C) demonstrated similar features as observed for fraction **N1** (Figure 2B) and the N-glycan pool (Figure 2A), including the Neu5Ac(α2-6), Fuc(α1-6), and GlcNAc(α1-*P*)Man structural-reporter groups, but only a trace amount of Fuc(α1-3) could be observed.

Preparative HPLC separation of di-charged FPLC fraction **N2** on LiChrosorb-NH_2 yielded four fractions, denoted **N2.1**–**N2.4** (Figure 4C). As evidenced by ^{1}H NMR analysis, all fractions contained both Neu5Ac(α2-6) and GlcNAc (α1-*P*)Man elements, whereas fraction **N2.2** also contained (α1-6)-linked Fuc, and fraction **N2.4** both Fuc(α1-6) and Fuc(α1-3) elements. Fraction **N2.4** did not contain enough material (<2%) for further subfractionation. Subfractionations of fractions **N2.1**, **N2.2**, and **N2.3** were achieved via lectin affinity chromatography on agarose-bound SNA, as explained for fraction **N1** (see *Structural*

analysis of mono-charged N-glycans of N1), yielding **U** and **B** fractions. The various **U** and **B** fractions were investigated by ^{1}H NMR spectroscopy, and the structural-reporter-group data are listed in Tables IV and V, respectively. Full structures, including the numbering of the various residues, are depicted in Table VI.

MALDI-TOF MS analysis of **N2.1U**, **N2.2U**, and **N2.3U** showed pseudomolecular ions at m/z 2030.15, 2192.32, and 2355.36, respectively, correlating with the $[M\text{-}2H + 3Na]^+$ adducts of $Hex_6P_2GlcNAc_4$ ($M = 2029.53$), $Hex_7P_2GlcNAc_4$ ($M = 2191.59$) and $Hex_8P_2GlcNAc_4$ ($M = 2353.64$), respectively. Each of the three 2-AB labeled compounds showed only one signal by HPLC profiling.

The ^{1}H NMR spectrum of fraction **N2.1U** showed a close resemblance to that of **N1.2U**, with two major differences: a doubling of the intensity of the GlcNAc(α1-*P*) H-1 and NAc signals at δ 5.479 and 2.077, respectively, and upfield shifts for Man-**A** H-1 (Δδ −0.023 ppm) and Man-**4′** H-2 (Δδ −0.013 ppm). Taken together the various NMR data, it can be concluded that **N2.1U** is an extension of **N1.2U** with an extra GlcNAc(α1-*P*) unit at Man-**A**. Comparing all **U** fractions, it seems that GlcNAc-phosphorylation at O-6 of a Man residue leads to a clear upfield shift of its H-1 signal (Δδ −0.03 till −0.06 ppm).

Based on its ^{1}H NMR analysis, fraction **N2.2U** can be considered as an extension of **N1.3U.3** with one extra GlcNAc (α1-*P*-6) residue at Man-**C**, meaning that starting from **N0.7.1** (Man7) both Man-**B** and Man-**C** have such a substituent (GlcNAc H-1, δ 5.482; NAc, δ 2.076) (Figure 5C). Because of the noted shifts in δ value of several of the Man H-1 and H-2 signals, when going from neutral to GlcNAc-phosphorylated oligomannose-type structures, detailed 2D TOCSY (150 ms) and nuclear Overhauser enhancement spectroscopy (NOESY) (400 ms) experiments were carried out. NOESY cross-peaks between Man-**C** H-1 and Man-**4** H-2; Man-**A** H-1 and Man-**4′** H-3; Man-**B** H-1 and Man-**4′** H-6; and Man-**D3** H-1 and Man-**B** H-2; identified Man-**4**, -**4′**; -**A**, -**B**, -**C**, and -**D3**. These detailed assignments, together with the literature NMR data by Nimtz et al. (1995) for **N1.2U**, have been used in the identification of the various Man residues in the other GlcNAc-phosphorylated compounds. Application of 2D ^{31}P selected ^{1}H-^{1}H NMR spectroscopy (Figure 7) confirmed the so far suspected GlcNAc(α1-*P*-6)Man linkages (GlcNAc H-1, δ 5.482; Man H-6a, δ 4.125; Man H-6b, δ 3.959). Going from **N0.7.1** to **N2.2U**, clear upfield shifts are detected for Man-**B** H-1 (Δδ −0.050 ppm), Man-**C** H-1 (Δδ −0.029 ppm), and Man-**A** H-1 (Δδ −0.018 ppm). The relatively small upfield shift of Man-**A** H-1 (compare with **N2.1U**) is probably due to the GlcNAc-phosphorylation of both Man-**B** and Man-**C**.

The ^{1}H NMR data of fraction **N2.3U** reflected an extension of **N1.4U** with one extra GlcNAc(α1-*P*-6) residue at Man-**C**. Not only Man-**B** (H-1, Δδ −0.061 ppm) of **N0.8.2** (Man8′) is substituted by a GlcNAc(α1-*P*) element, but also Man-**C** (H-1, Δδ −0.033 ppm) (Figure 5D). The two GlcNAc(α1-*P*) H-1 and NAc signals coincide at δ 5.482, and 2.076, respectively. It is interesting to see that, comparing the ^{1}H NMR data of the different **U** fractions, coupling of a GlcNAc(α1-*P*) element at Man-**C** generally leads to a downfield shift of Man-**4** H-1 of approximately Δδ +0.020 ppm. Finally, the precise position of the GlcNAc-phosphorylated Man-**B** H-1 signal seems to be dependent on the presence or absence of a GlcNAc(α1-*P*) element at Man-**C**: going from **N1.4U** to **N2.3U** Man-**B** H-1 shows an upfield shift of Δδ −0.017 ppm, whereas going from **N1.3U.3** to **N2.2U** this upfield shift is Δδ −0.013 ppm.

MALDI-TOF MS analysis of fractions **N2.1B** and **N2.2B** showed pseudomolecular ions at m/z 2290.18 and 2436.79, correlating with the $[M\text{-}2H + 3Na]^+$ adducts of $Neu5Ac_2Hex_5GlcNAc_4$ ($M = 2289.74$) and $Neu5Ac_2Hex_5Fuc_1GlcNAc_4$ ($M = 2435.98$), respectively. HPLC profiling on 2-AB labeled **N2.1B** and **N2.2B** confirmed the presence of only one structure in each fraction. The ^{1}H NMR data of fraction **N2.1B** are in accordance with a conventional nonfucosylated, (α2-6)-disialylated diantennary complex-type carbohydrate chain (cf. N2.3 in Damm et al. 1989, and Q2.4 in van Rooijen et al. 1998). Those of fraction **N2.2B** are in agreement with a conventional (α1-6)-fucosylated, (α2-6)-disialylated diantennary N-glycan (cf. Q2.2 in van Rooijen et al. 1998).

MALDI-TOF MS analysis of fraction **N2.3B** indicated a major pseudomolecular ion at m/z 2403.44, corresponding with the $[M\text{-}2H + 3Na]^+$ adduct of $Neu5Ac_1Hex_7PGlcNAc_4$ ($M = 2402.71$). The ^{1}H NMR spectrum revealed **N2.3B** to be a hybrid-type N-glycan with an (α2-6)-linked Neu5Ac in the Man(α1-3) arm (Man-**4** H-1, δ 5.123), and four Man residues, of which one bears a GlcNAc(α1-*P*-6) substituent in the Man(α1-6) arm (Man-**4′** H-1, δ 4.876). The Man-**B** H-1 signal resonates at δ 5.113, thereby indicating that Man-**B** bears the GlcNAc(α1-*P*-6) elongation (compare with **N1.3U.3**).

MALDI-TOF MS analysis of **N2.4** revealed pseudomolecular ions at m/z 2994.87 and 2567.89, correlating with the $[M\text{-}2H + 3K]^+$ adducts of $Neu5Ac_2Hex_6Fuc_2HexNAc_5$ ($M = 2994.91$), and $Hex_9P_2GlcNAc_4$ ($M = 2563.61$), respectively. The ^{1}H NMR spectrum of fraction **N2.4** revealed indications for an (α1-6)-fucosylated, (α2-6)-sialylated complex-type N-glycan with a Lewis x epitope, as well as a GlcNAc-phosphorylated oligomannose-type structure.

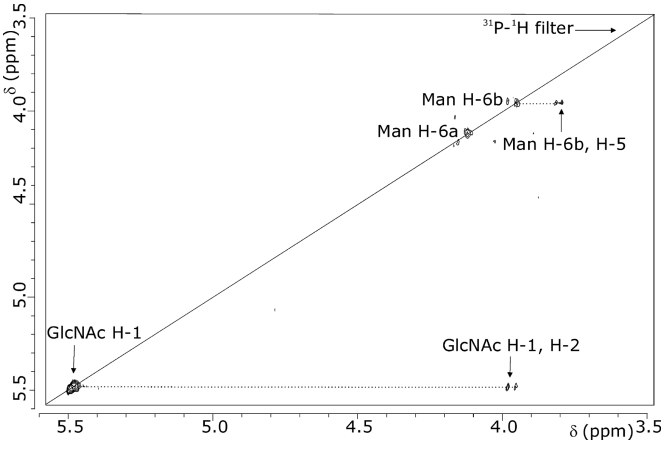

Fig. 7. Partial ^{31}P-filtered two-dimensional ^{1}H-^{1}H TOCSY spectrum of fraction **N2.2U** at 500 MHz recorded with a MLEV-17 mixing time of 10 ms. Peaks on the diagonal originate from the filter selection on the ^{31}P–^{1}H coupling. Cross peaks (nonsymmetrical) occur due to TOCSY transfer of the ^{31}P-filtered signal on the diagonal (TOCSY transfers are visible on horizontal lines in the spectrum: dashed lines).

Site specificity studies

Liquid chromatography tandem mass spectroscopy (LC/MS) peptide map analysis of the site specific glycosylation

Table VII. Mass spectrometry site specificity data performed on rhAGLU[a]

Site	rhAGLU composition		Fraction
Asn-140	$Neu5Ac_1Hex_7PHexNAc_4$	(Hybrid 1(*P*)GN)	**N2.3B**
	$Hex_7P_2HexNAc_4$	($M7(P)_2GN_2$)	**N2.2U**
	$Hex_7P_2HexNAc_3$	($M7(P)_2GN$)	
	$Neu5Ac_2Hex_5Fuc_1HexNAc_4$	(Complex A)	**N2.2B**
Asn-233	$Hex_7HexNAc_2$	(M7)	**N0.7.1**, **N0.7.2**, and/or **N0.7.3**
	$Hex_8HexNAc_2$	(M8)	**N0.8.1**, **N0.8.2**, and/or **N0.8.3**
	$Hex_6HexNAc_2$	(M6)	**N0.6.1** and/or **N0.6.2**
	$Hex_7PHexNAc_3$	(M7(*P*)GN)	**N1.3U.1**, **N1.3U.2**, and/or **N1.3U.3**
	$Hex_9PHexNAc_3$	(M9(*P*)GN)	
	$Hex_8PHexNAc_3$	(M8(*P*)GN)	**N1.4U**
Asn-390	$Hex_5HexNAc_2$	(M5)	**N0.5**
	$Hex_6HexNAc_2$	(M6)	**N0.6.1** and/or **N0.6.2**
	$Hex_7HexNAc_2$	(M7)	**N0.7.1**, **N0.7.2**, and/or **N0.7.3**
Asn-470	$Hex_8PHexNAc_3$	(M8(*P*)GN)	**N1.4U**
	$Hex_5HexNAc_2$	(M5)	**N0.5**
	$Hex_6HexNAc_2$	(M6)	**N0.6.1** and/or **N0.6.2**
	$Neu5Ac_1Hex_6HexNAc_3$	(Hybrid 2)	
	$Hex_8PHexNAc_2$	(M8(*P*))	
	$Hex_7PHexNAc_3$	(M7(*P*)GN)	**N1.3U.1**, **N1.3U.2**, and/or **N1.3U.3**
	$Hex_6PHexNAc_2$	(M6(*P*))	
	$Hex_4HexNAc_2$	(M4)	
	$Hex_6PHexNAc_3$	(M6(*P*)GN)	**N1.2U**
	$Hex_7HexNAc_2$	(M7)	**N0.7.1**, **N0.7.2**, and/or **N0.7.3**
	$Hex_3HexNAc_2$	(M3)	
	$Hex_7PHexNAc_2$	(M7(*P*))	
Asn-652	$Neu5Ac_1Hex_6HexNAc_3$	(Hybrid 2)	
	$Hex_5HexNAc_2$	(M5)	**N0.5**
	$Neu5Ac_1Hex_5HexNAc_3$	(Hybrid 4)	**N1.2B**
	$Neu5Ac_1Hex_4HexNAc_3$	(Hybrid 3)	**N1.1**
	$Neu5Ac_2Hex_5HexNAc_4$	(Complex B)	**N2.1B**
	$Neu5Ac_1Hex_7HexNAc_3$	(Hybrid 1)	
	$Neu5Ac_1Hex_5Fuc_1HexNAc_4$	(Complex C)	**N1.3B**
	$Neu5Ac_2Hex_5Fuc_1HexNAc_4$	(Complex A)	**N2.2B**
	$Neu5Ac_1Hex_5Fuc_2HexNAc_4$	(Complex D)	**N1.4B**
Asn-882	$Neu5Ac_2Hex_5Fuc_1HexNAc_4$	(Complex A)	**N2.2B**
	$Neu5Ac_1Hex_5Fuc_2HexNAc_4$	(Complex D)	**N1.4B**
	$Neu5Ac_1Hex_5Fuc_1HexNAc_4$	(Complex C)	**N1.3B**
	$Neu5Ac_2Hex_5HexNAc_4$	(Complex B)	**N2.1B**
Asn-925	$Neu5Ac_2Hex_5Fuc_1HexNAc_4$	(Complex A)	**N2.2B**
	$Neu5Ac_1Hex_5Fuc_2HexNAc_4$	(Complex D)	**N1.4B**
	$Neu5Ac_2Hex_5HexNAc_4$	(Complex B)	**N2.1B**
	$Neu5Ac_1Hex_5Fuc_1HexNAc_4$	(Complex C)	**N1.3B**

[a]The abbreviations between brackets have been used in Figure 8.

(Table VII and Figure 8) demonstrated a glycoform heterogeneity comparable to that observed by ^{1}H NMR and MALDI-TOF MS experiments. Site specific glycosylation patterns were determined for all seven N-linked sites. Phosphorylated oligomannose- or hybrid-type structures were found at three of the seven sites, namely, Asn-140, Asn-233, and Asn-470. The majority of the phosphorylated oligomannose-type N-glycans was capped by a terminal GlcNAc group. A small amount of noncapped glycans were also observed. Remarkably, Asn-882 and Asn-925 were only occupied by complex-type N-glycans with varying degrees of sialylation. The accurate mass measurement capability of the Q-STAR qq-TOF MS system made it possible to differentiate the 1 Da mass difference between a diantennary/difucosylated/monosialylated glycan and a diantennary/disialylated glycan. The observed HPLC retention shift between the two glycoforms is also in agreement of the charge difference between them. The detection of the diantennary/difucosylated/monosialylated glycan confirms the existence of Fuc(α1-3) in addition to core-Fuc(α1-6), proposed by the ^{1}H NMR data.

Discussion

In the literature so far only detailed glycan studies are available for native placental human GAA (Mutsaers et al. 1987), constituting the two active forms with molecular masses of 76 and 70 kDa. The 76-kDa form contains five and the 70-kDa form contains four N-glycosylation sites. Using ^{1}H NMR spectroscopy, it was found that the oligomannose-type N-glycans present were of intermediate size, $Man_5GlcNAc_2$ and $Man_7GlcNAc_2$ (missing Man-**D1** and Man-**D2**), and of small size, $Man_3GlcNAc(Fuc_{0-1})GlcNAc$ and $Man_2GlcNAc(Fuc_{0-1})GlcNAc$ (missing Man-**4**). Furthermore, a tiny amount of sialylated diantennary N-glycans was detected. No indications for phosphorylation were found.

Here, we focus on the glycosylation pattern of rhAGLU, expressed in the mammary gland of transgenic rabbits and excreted in the milk. The methodologies applied comprised monosaccharide analysis, mass spectrometry, ^{1}H and ^{31}P NMR spectroscopy, and HPLC-profiling/exoglycosidases. The structural results for rhAGLU show a highly complex N-glycosylation pattern, consisting of neutral oligomannose-type, GlcNAc-phosphorylated oligomannose-type, (α2-6)-monosialylated [(α1-6)-fucosylated] hybrid- and diantennary complex-type, (α2-6)-disialylated [(α1-6)-fucosylated] diantennary complex-type, and monosialylated GlcNAc-phosphorylated hybrid-type N-glycans. Four of the complex-type N-glycans were also shown to contain the Lewis x epitope. In addition trace amounts of glycans with an extra antenna on the Man(α1-3) arm seem to be present. Sialic acid analysis demonstrated only trace amounts of *N*-glycolylneuraminic acid. The site-specificity studies indicated heterogeneous patterns for each of the seven N-glycosylation sites. It is interesting to note that only Asn-140, Asn-233, and Asn-470 contained phosphorylated oligomannose- and hybrid-type structures, whereas Asn-882 and Asn-925 were only occupied by complex-type N-glycans. No indications for O-glycosylation were found.

In rhAGLU, the endo-mannosidase pathway is competitively active (Moore and Spiro 1990), just like in the earlier discussed case of recombinant human C1 inhibitor, expressed in the milk of transgenic rabbits (Koles, van Berkel, Pieper,

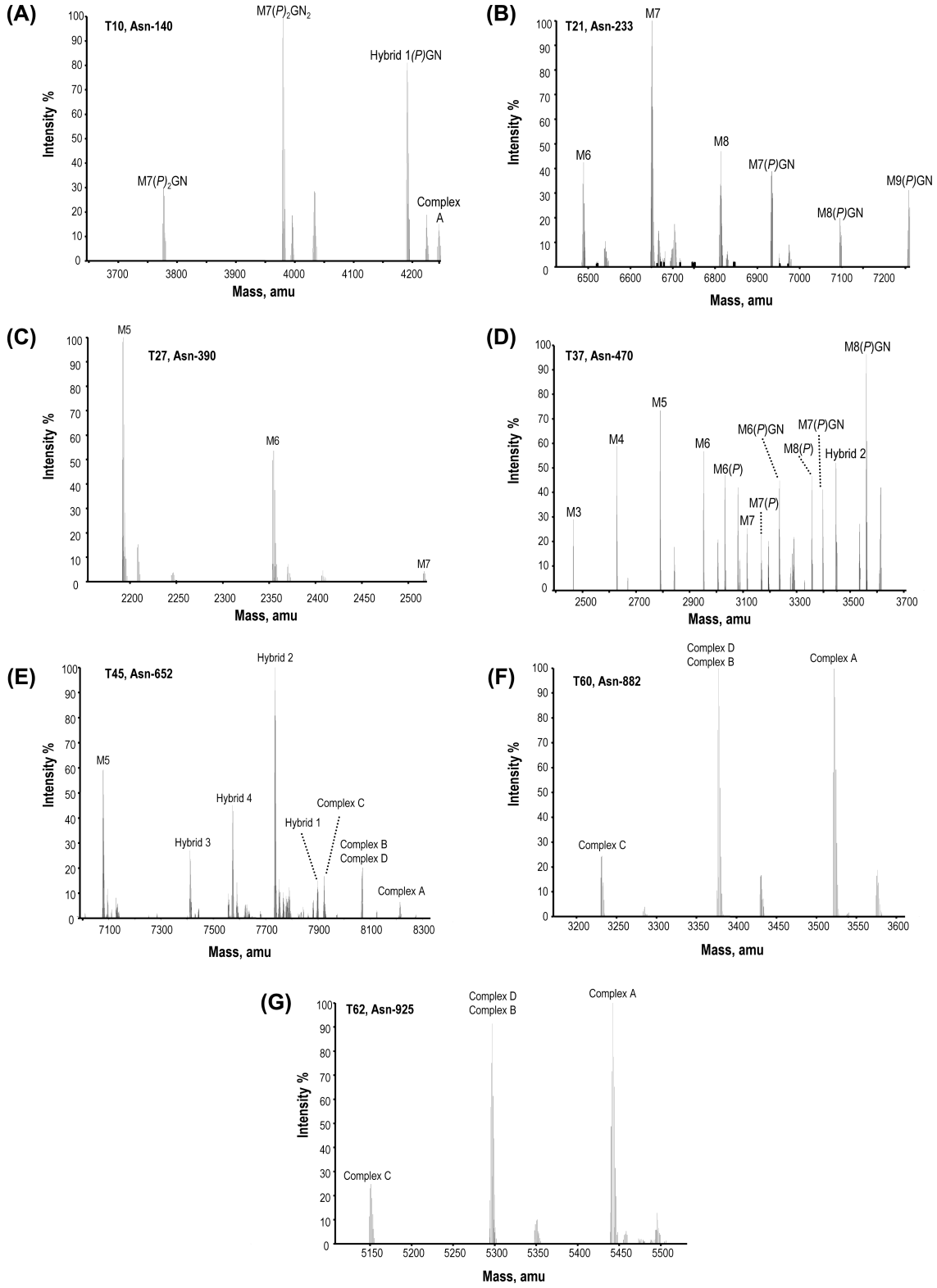

Fig. 8. Mass spectra of the glycopeptides of the seven N-glycosylation sites stemming from the site-specificity studies. (**A**) Asn-140; (**B**) Asn-233; (**C**) Asn-390; (**D**) Asn-470; (**E**) Asn-652; (**F**) Asn-882; and (**G**) Asn-925. For the coding system, see Table VII.

et al. 2004; Koles, van Berkel, Mannesse, et al. 2004). Inspection of the structures in the neutral fraction **N0** (Table III) shows the presence of the three possible $Man_8GlcNAc_2$ isomers, namely, Man8 (major normal pathway; absence of Man-**D2**), Man8′ (endo-mannosidase pathway; absence of Man-**D1**), and Man8″ (minor normal pathway; absence of Man-**D3**) (Weng and Spiro 1993, 1996; Verbert 1995; Ermonval et al. 2001). Additionally, the three

isomers of $Man_7GlcNAc_2$ occur, with Man7 being the most abundant one, as well as the two isomers of $Man_6GlcNAc_2$, one with Man-**C** (Man6) and one with Man-**D2** (Man6′). The smallest glycan is $Man_5GlcNAc_2$ (Man5).

Inspection of the various GlcNAc-phosphorylated $Man_{6-9}GlcNAc_2$ and hybrid-type N-glycans indicates that the major structures are derived from $Man_{6-8}GlcNAc_2$, missing Man-**D1**. The GlcNAc(α1-*P*-6) units occur at Man-**A**, Man-**B** when substituted with Man-**D3**, and/or Man-**C**. No indications for phosphorylation were observed for Man-**D1**, Man-**D2**, and Man-**D3**. Previously, Varki and Kornfeld (1980) reported that GlcNAc(α1-*P*-6) units (one or two) can occur on Man-**A** when missing Man-**D2**, Man-**B,** Man-**C**, Man-**D1**, and/or Man-**D3** of $Man_{6-9}GlcNAc_2$ structures, as specified for β-glucuronidase from mouse lymphoma cells. Even the hybrid-type structure **N2.3B** has been detected in $P388D_1$ mouse macrophage cells (Varki and Kornfeld 1983).

A unique event in the N-glycosylation of lysosomal enzymes is the mannose 6-phosphorylation. In this process, first, UDP-*N*-acetylglucosamine:glycoprotein *N*-acetylglucosamine-1-phosphotransferase (EC 2.7.8.17) transfers GlcNAc(α1-*P*) from UDP-GlcNAc to one or more mannose residues on lysosomal enzymes to give rise to a phosphodiester intermediate (Reitman and Kornfeld 1981a, 1981b; Waheed et al. 1982). Then, the *N*-acetylglucosamine-1-phosphodiester α-*N*-acetylglucosaminidase (EC 3.1.4.45), the uncapping enzyme, removes the GlcNAc residue to generate the active phosphomonoester (Varki and Kornfeld 1981; Waheed et al. 1981; Varki and Marth 1999). The free phosphate(s) can now be targeted by the MPR and transported towards the lysosomes. "Capped" phosphates cannot be targeted and no transport towards the lysosomes can occur via this way.

Detailed structural analysis of the glycosylation patterns of recombinant therapeutic glycoproteins is a prerequisite for their reliable use in patients. Undesirable immunogenic effects should be eliminated or at least reduced to a minimum. From phase I and phase II clinical trials, it is known that the transgenic human GAA (rhAGLU), described in this paper, is well accepted by patients with Pompe disease (van den Hout et al. 2000; van den Hout et al. 2001; van den Hout et al. 2004; Winkel et al. 2004; Klinge, Straub, Neudorf, Schaper, et al. 2005; Klinge, Straub, Neudorf, Voit, 2005). Evaluating the N-glycosylation pattern of the transgenic product, conventional oligomannose-, hybrid-, and complex-type N-glycans, regularly found in human glycoproteins are present. Neu5Gc, which may lead to immune reactions in humans, is only present in trace amounts. The major difference with the N-glycosylation of native lysosomal enzymes is the occurrence of capped phosphate groups (GlcNAc(α1-*P*-6)Man) (27% of the total glycan pool) on part of the oligomannose- and hybrid-type structures. Indications for the presence of very minor amounts of noncapped phosphate groups in different rhAGLU batches were obtained from the included MS site-specificity studies as well as from in vitro experiments (A.J.J. Reuser et al. unpublished results). As discussed already, Man6*P* constituents are essential to be targeted by the MPR in order to reach the lysosomes (Gabel and Kornfeld 1982; Goldberg and Kornfeld 1983; Kornfeld and Kornfeld 1985; Kornfeld 1986). So, theoretically, taking into account the N-glycosylation pattern of rhAGLU, the recombinant product should be biologically inactive. However, the clinical trials have shown that it is biologically active after intravenous injection in patients (*vide infra*). Previously, it has been reported that, although *N*-acetylglucosamine-1-phospho-diester α-*N*-acetylglucosaminidase resides in the *trans*-Golgi network (TGN), it cycles between the TGN and the plasma membrane, and is partially available at the cell surface (Kornfeld and Mellman 1989; Rohrer and Kornfeld 2001). Moreover, it has been demonstrated that human serum contains free *N*-acetylglucosamine-1-phospho-diester α-*N*-acetylglucosaminidase, suggested to be derived from the Golgi enzyme (Lee and Pierce 1995). A possible explanation is that rhAGLU is uncapped in the bloodstream, then targeted by the MPR and transported towards the lysosome, starting the glycogen clearance. Following this assumption, it means that rhAGLU can be considered as a predrug, becoming fully biologically active after in vivo processing by endogenous enzymatic pathways. In this context, the finding of two GlcNAc-phosphorylated Man residues per glycan in rhAGLU is important, because diphosphorylated glycans are better recognized by the MPR than monophosphorylated ones (Goldberg and Kornfeld 1981; Natowicz et al. 1982).

Materials and methods

Recombinant human acid α-glucosidase

rhAGLU, isolated and purified from pooled milk of a transgenic rabbit line expressing the glycoprotein on a 8 g/l scale (Bijvoet et al. 1999), was obtained from Pharming Technologies BV, Leiden, The Netherlands.

Release and isolation of N-linked glycans

Purified rhAGLU (70 mg) was dissolved in 5 ml 50 mM sodium phosphate buffer pH 7.3, containing 10 mM EDTA, 10 mM β-mercaptoethanol, and 0.5% SDS (w/v), then denaturated for 5 min at 100°C. After having added Nonidet P40 (Sigma, Zwijndrecht, The Netherlands) to a final concentration of 1.5% (v/v), the N-glycans were released with recombinant PNGase F (from *Flavobacterium meningosepticum* expressed in *Escherichia coli*, EC 3.5.1.52; Roche Molecular Biochemicals, Indianapolis, IN). The digestion was carried out with 350 U PNGase F (added in two steps: 250 U at t_0 and 100 U after 12 h) for 24 h at 37°C. After filtration through 30-kDa cut-off centrifugal filters (Nalgene, Neerijse, Belgium), the de-N-glycosylated glycoprotein was recovered from the filters, and checked by SDS-PAGE (Laemmli 1970) and monosaccharide analysis (Kamerling and Vliegenthart 1989). The filtrate, containing the released N-glycans, was treated with Calbiosorb Adsorbent (Calbiochem, San Diego, CA) according to the manufacturer's protocol to remove detergents. Finally, the N-glycan pool was desalted and purified on a Bio-Gel P-2 column (43 × 1.5 cm, Bio-Rad Laboratories, Veenendaal, The Netherlands), eluted with 10 mM NH_4HCO_3, followed by lyophilization.

Monosaccharide analysis

Glycan (glycoprotein) samples were subjected to methanolysis (1.0 M methanolic HCl, 24 h, 85°C) followed by re-N-acetylation and trimethylsilylation (Kamerling and Vliegenthart

1989). The mixture of trimethylsilylated (methyl ester) methyl glycosides was analyzed by gas-liquid chromatography (GLC) on an EC-1 column (30 m x 0.32 mm, Alltech, Breda, The Netherlands), using a Chrompack CP 9002 instrument (Chrompack, Middelburg, The Netherlands), and applying a temperature program of 140–240°C at 4°C/min. Confirmation of the data was established via combined GLC-EIMS on a GC 8060/MD 800 system (Fisons Instruments/Interscience, Breda, The Netherlands), equipped with an AT-1 column (30 m × 0.25 mm, Alltech), using the same temperature program as for GLC.

Sialic acid determination

Glycan (glycoprotein) samples were subjected to sialic acid analysis (Hara et al. 1989). Briefly, aliquots (10 μg) were hydrolyzed in 200 μl 2 M acetic acid for 3 h at 80°C. After cooling to room temperature, 200 μl of a 1,2-diamino-4,5-methylene-dioxybenzene (DMB) solution was added, and the samples were heated in the dark at 50°C for 2.5 h. The DMB solution was prepared by dissolving 3 mg DMB in 1898.1 μl of a solution prepared by mixing 6 mg sodium hydrosulfite, 100.8 μl β-mercaptoethanol, 1340.4 μl 2 M acetic acid, and 472.8 μl water. After cooling on ice, the generated DMB derivatives of sialic acids were immediately analyzed on a reversed-phase Cosmosil 5C18-AR-II column (4.6 × 250 mm, Waters, Eschborn, Germany), using a Spectroflow 400 HPLC system (ABI Analytical Kratos Division, Separations, H.I. Ambacht, The Netherlands), equipped with a Spectroflow 980 fluorescence detector ($\lambda_{exc.max} = 373$ nm, $\lambda_{em.max} = 448$ nm). The elution was carried out isocratically, using acetonitrile:methanol:water (9:7:84, v/v) as solvent.

Anion-exchange chromatography on Resource Q

The N-glycan pool of rhAGLU was fractionated into neutral and charged species on a Resource Q column (6 ml, Pharmacia, Uppsala, Sweden), using a Pharmacia FPLC system. The column was first eluted with water, followed by a linear concentration gradient of 0–0.5 M NaCl, at a flow rate of 4 ml/min; for gradient details, see Figure 3. The elution was monitored by UV absorbance at 214 nm. Individual fractions were lyophilized, then desalted on a Bio-Gel P-2 column (44 × 1 cm) using 10 mM NH_4HCO_3 as eluent, and lyophilized again.

HPLC fractionation on LiChrosorb-NH_2

The FPLC fractions were further fractionated on a LiChrosorb-NH_2 10 μm column (250 mm × 4.6 mm, Alltech), connected with a LiChrospher Amino 5 μm guard column (7.5 × 4.6 mm), using a Waters 600 HPLC system. A 50-min gradient of water or 10 mM potassium phosphate buffer, pH 6.5, in acetonitrile (each 20–45%, v/v), at a flow rate of 2 ml/min, was used; for gradient details see Figure 4A–C. The fractionations were monitored by UV absorbance at 206 nm, and the individual fractions were lyophilized without desalting.

Labeling of N-glycans with 2-AB and HPLC profiling

Purified and lyophilized N-glycans were treated with 0.35 M 2-AB/1 M sodium cyanoborohydride in dimethyl sulfoxide: acetic acid (7:3, v/v) for 2 h at 65°C. The 2-AB labeled glycans were purified via paper chromatography on acid-pretreated QMA (Whatman) filter paper strips using acetonitrile (three times) as a mobile phase. Glycans (remaining at the base line) were eluted from the dried paper strips with water, and concentrated (Bigge et al. 1995; Kinoshita and Sugahara 1999).

Profiling was carried out on a GlycoSep-N column (50 × 4.6 mm, Oxford GlycoScience, Oxford, UK) at 30°C, using a Waters 2690XE Alliance system, equipped with a Waters 474 fluorescence detector ($\lambda_{exc.max} = 373$ nm, $\lambda_{em.max} = 420$ nm). A 100-min gradient of 50 mM ammonium formate, pH 4.4, in acetonitrile (25.2–55%, v/v) was used, at a flow rate of 0.8 ml/min, followed by a 3-min gradient to 100% ammonium formate, which was kept for 5 min at 1 ml/min before regeneration started.

Exoglycosidase digestion of suitable amounts of dried 2-AB labeled fractions, as part of the HPLC profiling, were carried out for 18 h at 37°C in 20-μl solutions, containing 10 μl 0.1 M sodium citrate buffer, pH 5.3, and a fixed amount of enzyme solution completed with water to 10 μl. Before use, the 2-AB labeled samples were purified through 5-kDa cut-off centrifugal filters (Millipore, Amsterdam, The Netherlands). A 2-AB labeled dextran hydrolysate served as external calibration standard on GlycoSep-N. Incubations of oligomannose-type glycans were carried out with 3 μl jack bean α-mannosidase (19 U/ml, suspension in 3.0 M $(NH_4)_2SO_4$ and 0.1 M zinc acetate, pH 7.5; Sigma). Sequential and combined exoglycosidase digestions of hybrid- and complex-type glycans were carried out with 2 μl *Streptococcus pneumoniae* (α2-3)-sialidase (250 mU/ml, in 25 mM NaCl, 20 mM Tris–HCl, pH 7.5; Calbiochem); 2 μl *Arthrobacter* sialidase (1 U/100 μl, in 10 mM Na-phosphate, 0.1% Micr-O-protect, 0.25 mg/ml bovine serum albumin, pH 7; Roche); 3 μl bovine testis β-galactosidase (1–3 U/mg, suspension in 3.2 M $(NH_4)_2SO_4$, pH approximately 5.0; Sigma); 2 μl jack bean β-*N*-acetylglucosaminidase (50 U/mg, suspension in 2.5 M $(NH_4)_2SO_4$, pH 7.0; Sigma); and/or 3 μl jack bean α-mannosidase.

Mild acid hydrolysis/alkaline phosphatase digestion of phosphorylated glycans

Mild acid treatment of relevant samples was carried out in 100 mM HCl (0.5 ml) for 30 min at 100°C (Thieme and Ballou 1971). For dephosphorylation, samples, dissolved in 0.1 M NH_4HCO_3, were incubated overnight at 37°C with alkaline phosphatase (Sigma). Portions of 1 U/ml sample were added at $t = 0$ and at $t = 4$ h (Karson and Ballou 1978). Treatments were followed by HPLC profiling on a GlycoSep-N column, as described in *Labeling of N-glycans with 2-AB and HPLC profiling*.

Lectin affinity chromatography

Agarose-bound elderberry bark lectin (SNA) (2 ml; 3 mg lectin/ml gel) was obtained from Vector Laboratories (Burlingame, CA). After loading a small aliquot of the nondesalted mono- or di-charged HPLC LiChrosorb-NH_2 fractions in water onto the column (flow rate, 13 ml/h), the flow was stopped for about 15 min to achieve maximal binding; then, the column was washed with 20 ml PBS to elute the nonbinding fraction. The bound fraction [(α2-6)-sialylated N-glycans] was eluted with 20 ml 20 mM EDA, and the eluate was immediately neutralized with 4 M acetic acid. To elute eventual remaining material, the column was additionally eluted

with 20 ml 50 mM lactose. Re-equilibration to starting conditions was carried out with at least 70 ml PBS (Shibuya et al. 1987; Tai et al. 1992). All experiments were performed at 4°C. Individual SNA-binding and flow-through fractions were desalted on Carbograph SPE Ultra-Clean columns (150 mg, 4 ml; Alltech), and lyophilized.

NMR spectroscopy

Prior to ^{1}H NMR spectroscopy, samples were lyophilized three times from 99.9% $^{2}H_2O$ (Cambridge Isotope Laboratories Inc.). ^{1}H NMR spectra were recorded at 500 MHz on a Bruker DRX-500 instrument at a probe temperature of 300 K, or at 600 MHz on a Bruker Avance spectrometer with a cryo probe at 300 K (Bijvoet Center, Department of NMR Spectroscopy, Utrecht University).

One-dimensional 500 MHz ^{1}H spectra of 5000 Hz spectral widths were recorded in 8K complex data sets using a water eliminated Fourier transform pulse sequence as described by Hård et al. (1992). Chemical shifts are expressed in ppm relative to internal acetone (δ 2.225 in $^{2}H_2O$) (Vliegenthart et al. 1983).

Two-dimensional TOCSY spectra at 600 MHz were recorded using Bruker software with MLEV-17 mixing times of 70, 100, and 150 ms (Bax and Davis 1985a). Data matrices of 400 × 1024 points were collected representing a spectral width of 3004 Hz (5 ppm) in each dimension. The $^{2}HO^{1}H$ signal was suppressed by presaturation for 1 s during the relaxation delay.

Two-dimensional NOESY spectra at 600 MHz were recorded using Bruker software with a mixing time of 400 ms (Bax and Davis 1985a, 1985b). Data matrices of 512 × 1024 points were collected representing a spectral width of 5388 Hz (9 ppm) in each dimension. The $^{2}HO^{1}H$ signal was suppressed by presaturation for 1 s during the relaxation delay.

The ^{31}P-filtered two-dimensional ^{1}H-^{1}H TOCSY spectrum at 500 MHz was recorded with a MLEV-17 mixing time of 10 ms. ^{31}P-filtering using double INEPT was carried out with a selection delay of 30 ms on the small $^{31}P-^{1}H$ couplings.

Mass spectrometry

For MALDI-TOF MS in the positive-ion mode, neutral N-glycan samples (0.5–1 μl) were mixed in a 1:1 ratio with a solution of 10 mg 2,5-dihydroxybenzoic acid (DHB) in 1 ml 10 mM aqueous ethanol; charged N-glycan samples (0.5–1 μl) were mixed in a 1:1 ratio with a solution of 10 mg DHB in 1 ml 50% aqueous acetonitrile. For MS analysis in the negative-ion mode, 2′,4′,6′-trihydroxyacetophenone monohydrate in acetonitrile:13.3 mM ammonium citrate (1 : 3, v/v) (2 mg/ml) was used as a matrix. In this case, the sample-matrix mixture was dried under reduced pressure (Papac et al. 1998).

Neutral N-glycans were analyzed on a Voyager-DE MALDI-TOF mass spectrometer (Perseptive Biosystems, Framingham, MA) with implemented delayed extraction technique, using a VSL-337ND-N_2 laser (337 nm) with 3 ns pulse width. Spectra were recorded in the linear mode at an accelerating voltage of 24.5 kV, using an extraction delay of 90 ns. Mono- and di-charged N-glycans were analyzed on a Voyager-DE PRO MALDI-TOF mass spectrometer (Applied BioSystems, Foster City, CA), using a VSL-337ND-N_2 laser (337 nm) with 0.5 ns pulse width. Spectra were recorded in the reflector mode at an accelerating voltage of 20 kV, using an extraction delay of 95 ns. Found masses correlate within 1 mass unit with the calculated ones.

Preparation of peptide digests and LC/MS/MS analysis for site specificity studies

Site specificity data were collected on an earlier batch of rhAGLU. rhAGLU samples were diluted in 6 M guanidine-HCl/0.1 M Tris–HCl buffer, pH 8.5. The samples were reduced with 16.7 mM dithiothreitol at 55°C for 1 h in darkness, then cooled to room temperature, and alkylated with 0.39% 4-vinylpyridine at room temperature for 2 h in darkness. The reaction was stopped with 2 M dithiothreitol, and the samples were dialyzed using Slide-A-Lyser into 50 mM Tris–HCl buffer, pH 8.5, in a cold room. The derivatized rhAGLU samples were then treated with trypsin at a 1:50 enzyme protein ratio at 37°C overnight. The tryptic peptides were analyzed by capillary LC/MS/MS in a Q-STAR qq-TOF MS system (Applied Biosystems, Framingham, MA). Separations were carried out in a capillary Vydac C18 column (Microtech Scientific, 320 μm × 15 cm) with a 1% formic acid, acetonitrile gradient at a flow rate of 4 μl/min. The signals from all of the glycoforms at the same site were averaged and deconvoluted using Bioanalyst software and the individual glycoforms normalized based on peak areas.

Acknowledgements

We thank Dr R.W. Wechselberger for his help with the cryo 600 MHz NMR measurements and Prof. Dr. J.F.G. Vliegenthart for his interest.

Conflict of interest statement

None declared.

Abbreviations

2-AB, 2-aminobenzamide; DMB, 1,2-diamino-4,5-methylenedioxybenzene; EDA, ethylenediamine; FPLC, fast protein liquid chromatography; GAA, acid α-glucosidase; HPLC, high-performance liquid chromatography; LC/MS/MS, liquid chromatography tandem mass spectrometry; MALDI-TOF MS, matrix-assisted laser desorption ionization time-of-flight mass spectrometry; MLEV, composite pulse devised by M. Levitt; MPR, mannose 6-phosphate receptor; NMR, nuclear magnetic resonance; NOESY, nuclear Overhauser enhancement spectroscopy; PBS, phosphate buffered saline; PNGase F, peptide-N^4-(*N*-acetyl-β-glucosaminyl)asparagine amidase F; rhAGLU, recombinant human acid α-glucosidase; SPS–PAGE, sodium dodecyl sulfate–polacrylamide gel eletrophoresis; TGN, *trans*-Golgi network; TOCSY, total correlation spectroscopy

References

Bax A, Davis DG. 1985a. MLEV-17-based two-dimensional homonuclear magnetization spectroscopy. J Magn Reson. 65:355–360.

Bax A, Davis DG. 1985b. Practical aspects of two-dimensional transverse NOE spectroscopy. J Magn Reson. 63:207–213.

Bigge JC, Patel TP, Bruce JA, Goulding PN, Charles SM, Parekh RB. 1995. Nonselective and efficient fluorescent labeling of glycans using 2-amino benzamide and anthranilic acid. Anal Biochem. 230:229–238.

Bijvoet AGA, Kroos MA, Pieper FR, van der Vliet M, de Boer HA, van der Ploeg AT, Verbeet MP, Reuser AJJ. 1998. Recombinant human acid alpha-glucosidase: high level production in mouse milk, biochemical characteristics, correction of enzyme deficiency in GSDII KO mice. Hum Mol Genet. 7:1815–1824.

Bijvoet AGA, van Hirtum H, Kroos MA, van de Kamp EHM, Schoneveld O, Visser P, Brakenhoff JPJ, Weggeman M, van Corven EJ, van der Ploeg AT, et al. 1999. Human acid α-glucosidase from rabbit milk has therapeutic effect in mice with glycogen storage disease type II. Hum Mol Genet. 8: 2145–2153.

Damm JBL, Voshol H, Hård K, Kamerling JP, Vliegenthart JFG. 1989. Analysis of *N*-acetyl-4-*O*-acetylneuraminic-acid-containing N-linked carbohydrate chains released by peptide-N^4-(*N*-acetyl-β-glucosaminyl)asparagine amidase F. Application to the structure determination of the carbohydrate chains of equine fibrinogen. Eur J Biochem. 180:101–110.

de Waard P, Vliegenthart JFG, Kozutsumi Y, Kawasaki T, Yamashina I. 1989. Structural studies on phosphorylated oligosaccharides derived from yeast mannan by $^1H(^{31}P)$ relayed spin-echo difference spectroscopy (RESED). J Biol Chem. 264:12141–12144.

Ermonval M, Kitzmüller C, Mir AM, Cacan R, Ivessa NE. 2001. *N*-Glycan structure of a short-lived variant of ribophorin I expressed in the MadIA214 glycosylation-defective cell line reveals the role of a mannosidase that is not ER mannosidase I in the process of glycoprotein degradation. Glycobiology. 11:565–576.

Gabel CA, Kornfeld S. 1982. Lysosomal enzyme phosphorylation in mouse lymphoma cell lines with altered asparagine-linked oligosaccharides. J Biol Chem. 257:10605–10612.

Goldberg DE, Kornfeld S. 1981. The phosphorylation of β-glucuronidase oligosaccharides in mouse P388D1 cells. J Biol Chem. 256:13060–13067.

Goldberg DE, Kornfeld S. 1983. Evidence for extensive subcellular organization of asparagine-linked oligosaccharide processing and lysosomal enzyme phosphorylation. J Biol Chem. 258:3159–3165.

Guile GR, Rudd PM, Wing DR, Prime SB, Dwek RA. 1996. A rapid high-resolution high-performance liquid chromatographic method for separating glycan mixtures and analyzing oligosaccharide profiles. Anal Biochem. 240:210–226.

Gutiérrez Gallego R, Haseley SR, van Miegem VFL, Vliegenthart JFG, Kamerling JP. 2004. Identification of carbohydrates binding to lectins by using surface plasmon resonance in combination with HPLC profiling. Glycobiology. 14:373–386.

Hara S, Yamaguchi M, Takemori Y, Furuhata K, Ogura H, Nakamura M. 1989. Determination of mono-*O*-acetylated *N*-acetylneuraminic acids in human and rat sera by fluorometric high-performance liquid chromatography. Anal Biochem. 179:162–166.

Hård K, van Zadelhoff G, Moonen P, Kamerling JP, Vliegenthart JFG. 1992. The Asn-linked carbohydrate chains of human Tamm-Horsfall glycoprotein of one male. Novel sulfated and novel *N*-acetylgalactosamine-containing N-linked carbohydrate chains. Eur J Biochem. 209: 895–915.

Hasilik A, Neufeld EF. 1980. Biosynthesis of lysosomal enzymes in fibroblasts. Phosphorylation of mannose residues. J Biol Chem. 255: 4946–4950.

Hermans MM, Wisselaar HA, Kroos MA, Oostra BA, Reuser AJJ. 1993. Human lysosomal alpha-glucosidase: functional characterization of the glycosylation sites. Biochem J. 289 Pt 3:681–686.

Hirschhorn R, Reuser AJJ. 2001. Glycogen storage disease type II: acid alpha-glucosidase (acid maltase) deficiency. In: Scriver CR, Beaudet AC, Sly WS, Valle D, editors. The metabolic and molecular bases of inherited disease. 8th ed. New York (NY): McGraw-Hill; 3389–3420.

Kamerling JP, Vliegenthart JFG. 1989. Carbohydrates. In: Lawson MA, editor. Clinical biochemistry; principles, methods, applications, Vol. 1. Mass spectrometry. Berlin: Walter de Gruyter; 175–263.

Kamerling JP, Vliegenthart JFG. 1992. High-resolution ^1H-nuclear magnetic resonance spectroscopy of oligosaccharide-alditols released from mucin-type *O*-glycoproteins. In: Berliner LJ, Reuben J, editors. Biological magnetic resonance, vol. 10. New York (NY): Plenum Publishing Corporation; 1–194.

Kaplan A, Achord DT, Sly WS. 1977. Phosphohexosyl components of a lysosomal enzyme are recognized by pinocytosis receptors on human fibroblasts. Proc Natl Acad Sci USA. 74:2026–2030.

Karson EM, Ballou CE. 1978. Biosynthesis of yeast mannan. Properties of a mannosylphosphate transferase in *Saccharomyces cerevisiae.* J Biol Chem. 253:6484–6492.

Kinoshita A, Sugahara K. 1999. Microanalysis of glycosaminoglycan-derived oligosaccharides labeled with a fluorophore 2-aminobenzamide by high-performance liquid chromatography: application to disaccharide composition analysis and exosequencing of oligosaccharides. Anal Biochem. 269:367–378.

Kishnani PS, Nicolino M, Voit T, Rogers RC, Tsai AC-H, Waterson J, Herman GE, Amalfitano A, Thurberg BL, Richards S, et al. 2006. Chinese hamster ovary cell-derived recombinant human acid α-glucosidase in infantile-onset Pompe disease. J Pediatr. 149: 89–97.

Klinge L, Straub V, Neudorf U, Schaper J, Bosbach T, Gorlinger K, Wallot M, Richards S, Voit T. 2005. Safety and efficacy of recombinant acid alpha-glucosidase (rhGAA) in patients with classical infantile Pompe disease: results of a phase II clinical trial. Neuromuscul Disord. 15: 24–31.

Klinge L, Straub V, Neudorf U, Voit T. 2005. Enzyme replacement therapy in classical infantile Pompe disease: results of a ten-month follow-up study. Neuropediatrics. 36:6–11.

Koles K, van Berkel PHC, Mannesse MLM, Zoetemelk R, Vliegenthart JFG, Kamerling JP. 2004. Influence of lactation parameters on the N-glycosylation of recombinant human C1 inhibitor isolated from the milk of transgenic rabbits. Glycobiology. 14:979–986.

Koles K, van Berkel PHC, Pieper FR, Nuijens JH, Mannesse MLM, Vliegenthart JFG, Kamerling JP. 2004. N- and O-glycans of recombinant human C1 inhibitor expressed in the milk of transgenic rabbits. Glycobiology. 14:51–64.

Kornfeld R, Kornfeld S. 1985. Assembly of asparagine-linked oligosaccharides. Annu Rev Biochem. 54:631–664.

Kornfeld S. 1986. Trafficking of lysosomal enzymes in normal and disease states. J Clin Invest. 77:1–6.

Kornfeld S, Mellman I. 1989. The biogenesis of lysosomes. Annu Rev Cell Biol. 5:483–525.

Laemmli UK. 1970. Cleavage of structural proteins during the assembly of the head of bacteriophage T4. Nature 227:680–685.

Lee JK, Pierce M. 1995. Purification and characterization of human serum *N*-acetylglucosamine-1-phosphodiester α-*N*-acetylglucosaminidase. Arch Biochem Biophys. 319:413–425.

Michalski J-C, Haeuw J-F, Wieruszeski J-M, Montreuil J, Strecker G. 1990. In vitro hydrolysis of oligomannosyl oligosaccharides by the lysosomal α-D-mannosidases. Eur J Biochem. 189:369–379.

Moreland RJ, Jin X, Zhang XK, Decker RW, Albee KL, Lee KL, Cauthron RD, Brewer K, Edmunds T, Canfield WM. 2005. Lysosomal acid α-glucosidase consists of four different peptides processed from a single chain precursor. J Biol Chem. 280:6780–6791.

Moore SEH, Spiro RG. 1990. Demonstration that Golgi endo-α-D-mannosidase provides a glucosidase-independent pathway for the formation of complex N-linked oligosaccharides of glycoproteins. J Biol Chem. 265: 13104–13112.

Mutsaers JHGM, van Halbeek H, Vliegenthart JFG, Tager JM, Reuser AJJ, Kroos M, Galjaard H. 1987. Determination of the structure of the carbohydrate chains of acid α-glucosidase from human placenta. Biochim Biophys Acta. 911:244–251.

Natowicz M, Baenziger JU, Sly WS. 1982. Structural studies of the phosphorylated high mannose-type oligosaccharides on human beta-glucuronidase. J Biol Chem. 257:4412–4420.

Nimtz M, Wray V, Rüdiger A, Conradt HS. 1995. Identification and structural characterization of a mannose-6-phosphate containing oligomannosidic N-glycan from human erythropoietin secreted by recombinant BHK-21 cells. FEBS Lett. 365:203–208.

Oude Elferink RPJ, Brouwer-Kelder EM, Surya I, Strijland A, Kroos M, Reuser AJJ, Tager JM. 1984. Isolation and characterization of a precursor form of lysosomal α-glucosidase from human urine. Eur J Biochem. 139: 489–495.

Papac DI, Briggs JB, Chin ET, Jones AJS. 1998. A high-throughput microscale method to release N-linked oligosaccharides from glycoproteins for matrix-assisted laser desorption/ionization time-of-flight mass spectrometric analysis. Glycobiology. 8:445–454.

Reitman ML, Kornfeld S. 1981a. UDP-*N*-acetylglucosamine:glycoprotein *N*-acetylglucosamine-1-phosphotransferase. Proposed enzyme for the phosphorylation of the high mannose oligosaccharide units of lysosomal enzymes. J Biol Chem. 256:4275–4281.

Reitman ML, Kornfeld S. 1981b. Lysosomal enzyme targeting. *N*-Acetylglucosaminylphosphotransferase selectively phosphorylates native lysosomal enzymes. J Biol Chem. 256:11977–11980.

Reuser AJJ, Kroos MA, Hermans MMP, Bijvoet AGA, Verbeet MP, van Diggelen OP, Kleijer WJ, van der Ploeg AT. 1995. Glycogenosis type II (acid maltase deficiency). Muscle Nerve. 3, S61–S69.

Rohrer J, Kornfeld R. 2001. Lysosomal hydrolase mannose 6-phosphate uncovering enzyme resides in the *trans*-Golgi network. Mol Biol Cell. 12: 1623–1631.

Rudd PM, Dwek RA. 1997. Rapid, sensitive sequencing of oligosaccharides from glycoproteins. Curr Opin Biotechnol. 8:488–497.

Shibuya N, Goldstein IJ, Broekaert WF, Nsimba-Lubaki M, Peeters B, Peumans WJ. 1987. Fractionation of sialylated oligosaccharides, glycopeptides, and glycoproteins on immobilized elderberry (*Sambucus nigra L.*) bark lectin. Arch Biochem Biophys. 254:1–8.

Stroop CJM, Weber W, Gerwig GJ, Nimtz M, Kamerling JP, Vliegenthart JFG. 2000. Characterization of the carbohydrate chains of the secreted form of the human epidermal growth factor receptor. Glycobiology. 10:901–917.

Tai G-H, Morris HG, Brown GM, Huckerby TN, Nieduszynski IA. 1992. A sub-population of keratan sulphates derived from bovine articular cartilage is capped with α(2-6)-linked *N*-acetylneuraminic acid residues. Affinity chromatography using immobilized *Sambucus nigra* lectin and characterization using ^{1}H n.m.r. spectroscopy. Biochem J. 286:231–234.

Thieme TR, Ballou CE. 1971. Nature of the phosphodiester linkage of the phosphomannan from the yeast *Kloeckera brevis*. Biochemistry. 10: 4121–4129.

van den Hout HMP, Hop W, van Diggelen OP, Smeitink JAM, Smit GPA, Poll-The B-TT, Bakker HD, Loonen MCB, de Klerk JBC, Reuser AJJ, et al. 2003. The natural course of infantile Pompe's disease: 20 original cases compared with 133 cases from the literature. Pediatrics. 112:332–340.

van den Hout HMP, Reuser AJJ, Vulto AG, Loonen MCB, Cromme-Dijkhuis A, van der Ploeg AT. 2000. Recombinant human α-glucosidase from rabbit milk in Pompe patients. Lancet. 356:397–398.

van den Hout JMP, Kamphoven JHJ, Winkel LPF, Arts WFM, de Klerk JBC, Loonen MCB, Vulto AG, Cromme-Dijkhuis A, Weisglas-Kuperus N, Hop W, et al. 2004. Long-term intravenous treatment of Pompe disease with recombinant human α-glucosidase from milk. Pediatrics. 113:e448–e457.

van den Hout JMP, Reuser AJJ, de Klerk JBC, Arts WF, Smeitink JAM, van der Ploeg AT. 2001. Enzyme therapy for Pompe disease with recombinant human α-glucosidase from rabbit milk. J Inherit Metab Dis. 24:266–274.

van Rooijen JJM, Jeschke U, Kamerling JP, Vliegenthart JFG. 1998. Expression of N-linked sialyl Le^{X} determinants and O-glycans in the carbohydrate moiety of human amniotic fluid transferrin during pregnancy. Glycobiology. 8:1053–1064.

Varki A, Kornfeld S. 1980. Structural studies of phosphorylated high mannose-type oligosaccharides. J Biol Chem. 255:10847–10858.

Varki A, Kornfeld S. 1981. Purification and characterization of rat liver α-*N*-acetylglucosaminyl phosphodiesterase. J Biol Chem. 256:9937–9943.

Varki A, Kornfeld S. 1983. The spectrum of anionic oligosaccharides released by endo-β-*N*-acetylglucosaminidase H from glycoproteins. Structural studies and interactions with the phosphomannosyl receptor. J Biol Chem. 258:2808–2818.

Varki A, Marth J. 1999. N-glycans. In: Varki A, Cummings R, Esko J, Freeze H, Hart G, Marth J, editors. Essentials of glycobiology. Cold Spring Harbor (NY): Cold Spring Harbor Laboratory Press; 85–100.

Verbert A. 1995. Biosynthesis, 2b. From $Glc_3Man_9GlcNAc_2$-protein to $Man_5GlcNAc_2$-protein: transfer "en bloc" and processing. In Montreil J, Vliegenthart JFG, Schachter H, editors. Glycoproteins. Amsterdam: Elsevier Science BV; 145–152.

Vliegenthart JFG, Dorland L, van Halbeek H. 1983. High-resolution proton nuclear magnetic resonance spectroscopy as a tool in the structural analysis of carbohydrates related to glycoproteins. Adv Carbohydr Chem Biochem. 41:209–374.

Waheed A, Hasilik A, von Figura K. 1981. Processing of the phosphorylated recognition marker in lysosomal enzymes. Characterization and partial purification of a microsomal α-*N*-acetylglucosaminyl phosphodiesterase. J Biol Chem. 256:5717–5721.

Waheed A, Hasilik A, von Figura K. 1982. UDP-*N*-Acetylglucosamine: lysosomal enzyme precursor *N*-acetylglucosamine-1-phosphotransferase. Partial purification and characterization of the rat liver Golgi enzyme. J Biol Chem. 257:12322–12331.

Weng S, Spiro RG. 1993. Demonstration that a kifunensine-resistant α-mannosidase with a unique processing action on *N*-linked oligosaccharides occurs in rat liver endoplasmic reticulum and various cultured cells. J Biol Chem. 268:25656–25663.

Weng S, Spiro RG. 1996. Evaluation of the early processing routes of N-linked oligosaccharides of glycoproteins through the characterization of $Man_8GlcNAc_2$ isomers: evidence that endomannosidase functions *in vivo* in the absence of a glucosidase blockade. Glycobiology. 6:861–868.

Winkel LPF, van den Hout JMP, Kamphoven JHJ, Disseldorp JAM, Remmerswaal M, Arts WFM, Loonen MCB, Vulto AG, van Doorn PA, de Jong G, et al. 2004. Enzyme replacement therapy in late-onset Pompe's disease: a three-year follow-up. Ann Neurol. 55:495–502.

Wisselaar HA, Kroos MA, Hermans MMP, van Beeumen J, Reuser AJJ. 1993. Structural and functional changes of lysosomal acid α-glucosidase during intracellular transport and maturation. J Biol Chem. 268: 2223–2231.